Tectonics

RESEARCH ARTICLE
10.1029/2018TC005472

Geology of the Ionian Basin and Margins: A Key to the East Mediterranean Geodynamics

J. Tugend[1,2], N. Chamot-Rooke[1], S. Arsenikos[1], C. Blanpied[2], and D. Frizon de Lamotte[3]

[1]Laboratoire de Géologie, CNRS UMR 8538, Ecole normale supérieure, PSL Research University, Paris, France, [2]Sorbonne Université, CNRS-INSU, Institut des Sciences de la Terre Paris, ISTeP UMR 7193, Paris, France, [3]Département Géosciences et Environnement (GEC), Université de Cergy-Pontoise, Cedex, France

Key Points:
- We propose a coherent stratigraphic framework for the margins of the Ionian Basin using seismic data (Apulia, Malta, Sirte, and Cyrenaica)
- The age of the Ionian Basin is reevaluated to the Early-Middle Jurassic interval, following a Triassic-Lower Jurassic episode of rifting
- The Ionian Basin is a short-lived remnant resulting from the interaction between two propagating oceans, Central Atlantic and Neo-Tethys

Supporting Information:
- Supporting Information S1

Correspondence to:
J. Tugend,
julie.tugend@sorbonne-universite.fr

Citation:
Tugend, J., Chamot-Rooke, N., Arsenikos, S., Blanpied, C., & Frizon de Lamotte, D. (2019). Geology of the Ionian Basin and margins: A key to the East Mediterranean geodynamics. *Tectonics*, *38*, 2668–2702. https://doi.org/10.1029/2018TC005472

Received 27 DEC 2018
Accepted 17 JUN 2019
Accepted article online 2 JUL 2019
Published online 5 AUG 2019

Abstract We revisit the nature, structure, and evolution of the Ionian Basin and its surrounding passive margins (Apulia, Eastern Sicily/Malta, and Cyrenaica margins). Relying on geological observations (wells, dredges, and dives) and seismic calibrations from the surrounding platforms and escarpments, we present age correlations for the deepest sedimentary sequences of the Ionian Basin. Two-ship deep refraction seismic data combined with reprocessed reflection seismic data enable us to identify, characterize, and map these thick sedimentary sequences and to present a consistent seismic stratigraphy across the basin. At a larger scale, we present new geological transects illustrating the tectonostratigraphic relationships between the Ionian Basin and its surrounding rifted margins. On this basis, we suggest that a Late Triassic-Early Jurassic rifting preceded the late Early Jurassic to Middle Jurassic formation of the Ionian Basin. The combination of geophysical and geological arguments suggests that the entire deep basin is floored with oceanic crust of normal thickness, but with high seismic velocity in the upper part. Upscaling our results in the framework of the eastern Mediterranean, we propose that the Ionian Basin represents the remnant of a short-lived oceanic basin resulting from the interaction between two propagating oceans: the Central Atlantic and the Neo-Tethys.

1. Introduction

The origin of the deep East Mediterranean Basins (Levant, Herodotus, Sirte, and Ionian Basins, Figure 1) has been a long-lasting debate (e.g., Robertson, 2007, and references therein). A central question is the timing of formation of these deep basins in the general framework of the successive Tethys openings. The best structural and stratigraphic constraints are from the far east Levant margin (e.g., Ben-Avraham et al., 2002; Collin et al., 2010; Gardosh et al., 2010; Gardosh & Druckman, 2006; Garfunkel & Derin, 1984; Hawie et al., 2013; Steinberg et al., 2018) and Egyptian margin (e.g., Camera et al., 2010; Moustafa, 2008; Tari et al., 2012; Tassy et al., 2015; Yousef et al., 2010), which were thoroughly studied in the recent years because of their offshore petroleum potential. Several studies support the occurrence of polyphased rifting from Late Palaeozoic to Trias leading to extreme continental thinning (<10-km crust) in the Levant Basin and oceanic spreading in the Herodotus Basin in Early to Middle Jurassic time, with a preferred approximately NW-SE oriented extension (e.g., Barrier et al., 2008; Ben-Avraham et al., 2006; Frizon de Lamotte et al., 2011; Gardosh et al., 2010; Gardosh & Druckman, 2006; Garfunkel, 1998, 2004; Garfunkel & Derin, 1984).

In contrast, the nature, age, and overall architecture of the Ionian Basin farther west are uncertain (Figure 1; syntheses in, e.g., Ben-Avraham et al., 2006, Catalano et al., 2001, Hieke et al., 2003, and Speranza et al., 2012) and relationships with easternmost basins (Levant) and even nearby adjacent basins (Sirte and Herodotus) remain unclear. The Ionian Sea was found to be floored with a thin crust (5–8 km) as early as the 1970s based on refraction measurements combined with gravity (Giese et al., 1982; Hinz, 1974). This led Finetti to conclude that "The Ionian abyssal basin is [...] a paleo-oceanic crust which has been continuously covered by deep water sediments from the Middle Jurassic to Quaternary" (Finetti, 1982). Although the depth to the Moho and the crustal thickness were confirmed by later studies (e.g., de Voogd et al., 1992; Dellong et al., 2018; Ferruci et al., 1991; Makris et al., 1986; Nicolich et al., 2000), the nature of the basement regularly comes into question mainly because indirect geophysical arguments failed to address the crucial question of the age of the basin: If the crust is oceanic, when did spreading occur and what was the ridge/transform system? If it is thinned continental crust, when did subsidence take place? Age estimates for the formation of the Ionian Basin (Figure 2) range from Carboniferous-

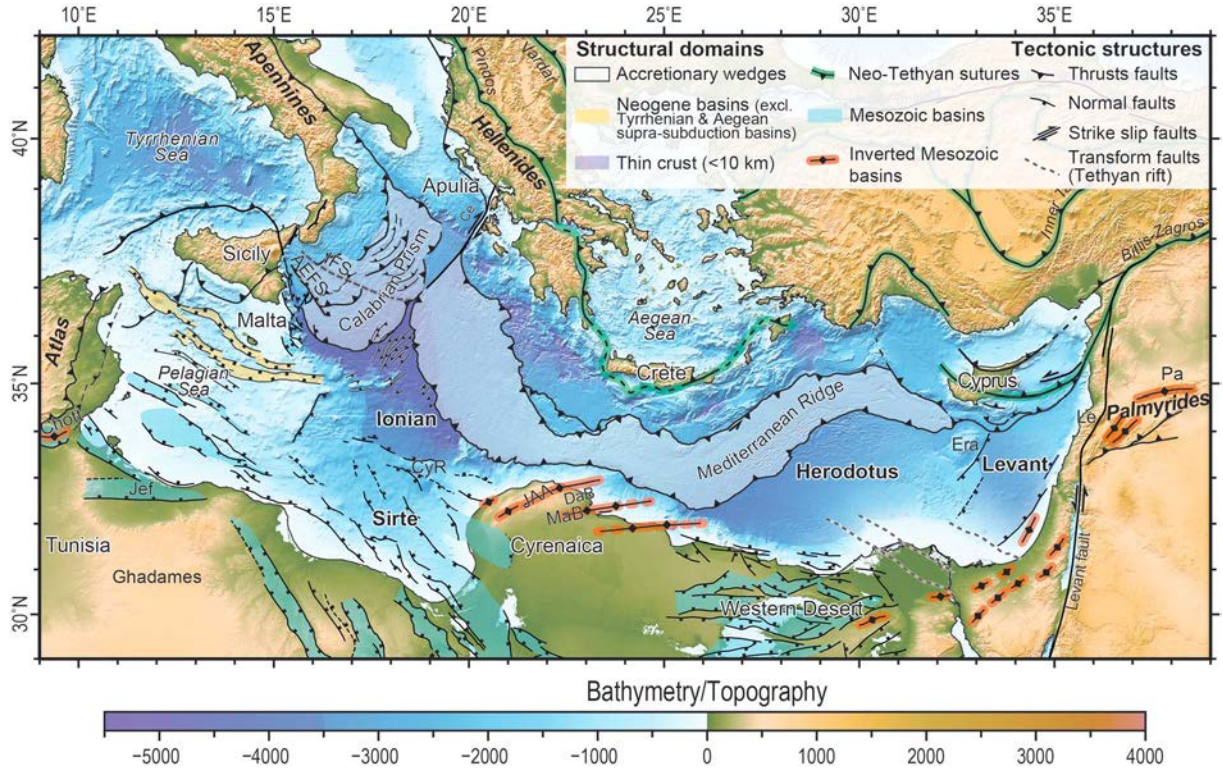

Figure 1. Simplified structural map of the eastern Mediterranean Basins. AEFA: Alfeo-Etna Fault system; Ce: Cephalonia Fault; CyR: Cyrenaica Ridge; DaB: Darnah Basin; Era: Eratosthenes; IFS: Ionian Fault System; JAA: Jabal Al Akhdar; Jef: Jeffara Basin; Le: Lebanon; MaB: Marmarica Basin; Pa: Palmyra through (after Arsenikos et al., 2013; Bosworth et al., 2008; Chamot-Rooke, Rangin, et al., 2005; Frizon de Lamotte et al., 2011; Gallais et al., 2011; Polonia et al., 2011, 2016, 2017; Robertson, 2007; Tassy et al., 2015, and own observations). Bathymetry from Becker et al. (2009).

Early Permian (e.g., Ben-Avraham & Ginzburg, 1990; Catalano et al., 1991; Granot, 2016; Vai, 2003) to Cretaceous (e.g., Chamot-Rooke, Rangin, et al., 2005; Dercourt et al., 1986, 1993), with a tendency to depart from the original Jurassic hypothesis of Finetti either toward the older ages (the eastern Mediterranean would then host the world's oldest oceanic crust) or younger ages (the entire deepening of the Ionian Sea would be Mio-Pliocene in age, which would still be a record in terms of the rate of subsidence). The direction of opening itself is an issue, since two orthogonal directions of extension have been suggested: either approximately NE-SW, as a southern branch of the Neo-Tethys ocean (e.g., Rosenbaum et al., 2004; Stampfli et al., 1991, 2001), or approximately NW-SE, concomitant with the Central Atlantic opening (e.g., Barrier et al., 2008; Chamot-Rooke, Rangin, et al., 2005; Frizon de Lamotte et al., 2011; Garfunkel, 1998, 2004). The Ionian Basin—opened at the junction between the European, African, and Apulian plates—thus appears as one of the key basins to constrain plate kinematic models in the wider framework of the evolution of the Neo-Tethys, Central Atlantic, and Alpine-Tethys oceans.

Here we compile marine geological observations using wells, dredges, and dives from the surrounding basins, platforms, and escarpments (Apulia, Eastern Sicily/Malta, and Cyrenaica margin segments and offshore Sirte Basin). We combine two-ship deep refraction seismic data (PASIPHAE cruise; Le Meur, 1997; Truffert et al., 1993; de Voogd et al., 1992) with a set of reprocessed reflection seismic profiles shot in the 1990s (ARCHIMEDE survey and International MEditerranean Ridge Seismic Experiment—IMERSE) to characterize and map sedimentary sequences across the Ionian Basin. Altogether, these data enable us to build new regional geological transects showing the structure and evolution of the Ionian Basin and its margins in the framework of the East Mediterranean.

2. The East Mediterranean Tectonic Setting

The East Mediterranean preserves the traces of a complex spatial and temporal succession of rift events that affected the North-Gondwana paleomargin from Palaeozoic to Mesozoic times. The main tectonic events

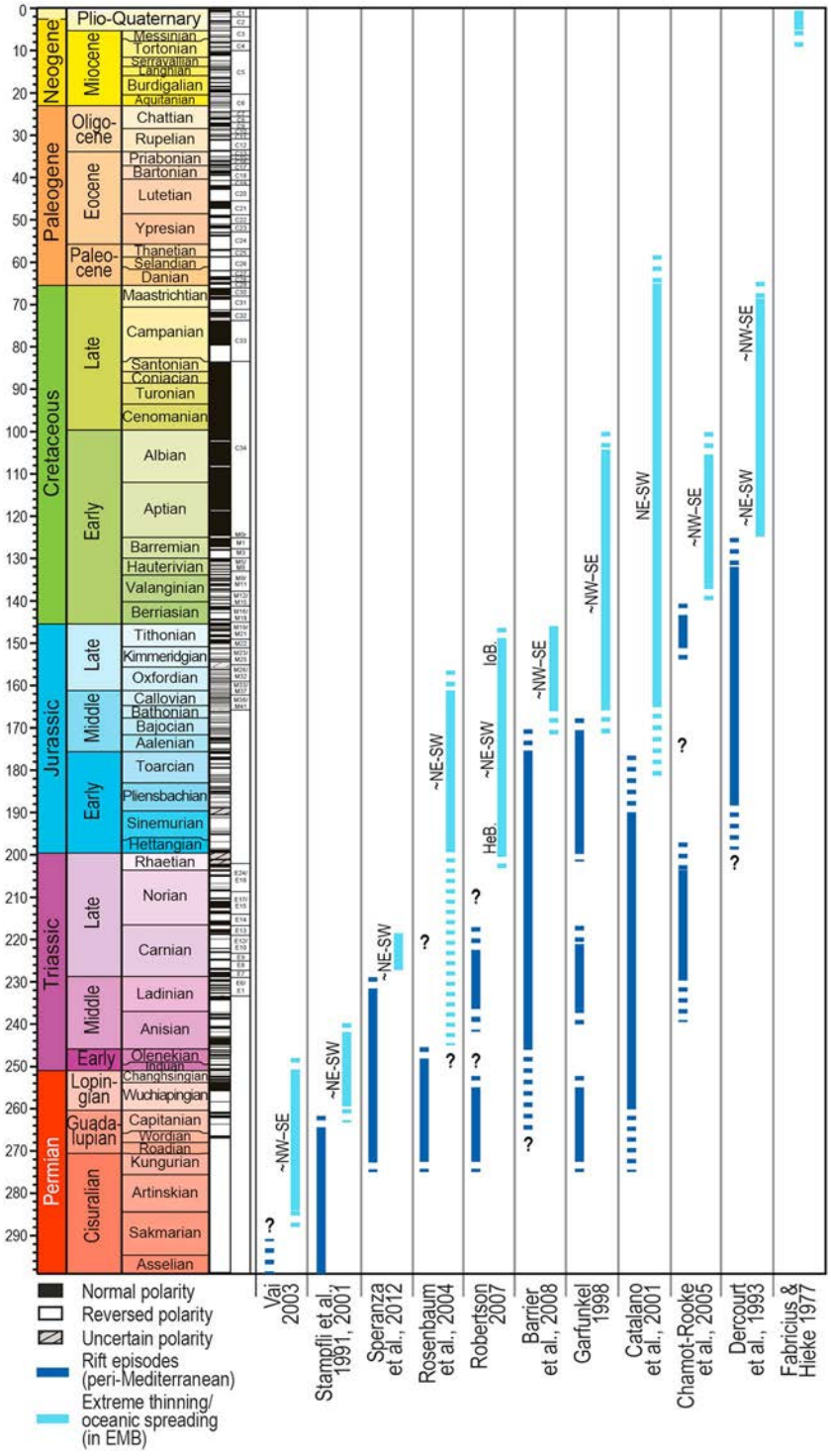

Figure 2. Diagram synthesizing the diversity of paleogeographic models and the implications for the age and opening directions of the East Mediterranean Basins (EMB; after Barrier et al., 2008; Catalano et al., 2001; Chamot-Rooke, Rangin, et al., 2005; Dercourt et al., 1993; Fabricius & Hieke, 1977; Robertson, 2007; Rosenbaum et al., 2004; Speranza et al., 2012; Stampfli et al., 1991, 2001; Vai, 2003). Conflicting ages are suggested, ranging from Early Permian to Miocene. Time scale from Gradstein and Ogg (2004).

that shaped the East Mediterranean domain are classically interpreted either as related to the Permian opening of the Neo-Tethys ocean (e.g., Schettino & Turco, 2011; Stampfli et al., 1991, 2001; Stampfli & Borel, 2002) or to a subsequent secondary branch that formed during Late Triassic to Early Jurassic (e.g., Barrier et al., 2008; Frizon de Lamotte et al., 2011; Garfunkel, 1998, 2004; Robertson, 2007; Robertson et al., 1996; Şengör, 1979; Şengör et al., 1984) or Late Jurassic to Cretaceous time (e.g., Catalano et al., 2001; Chamot-Rooke, Rangin, et al., 2005; Dercourt et al., 1986, 1993).

2.1. Geodynamic Scenarios: Geological and Paleomagnetic Constraints

Details of the geodynamic setting related to the formation and evolution of the East Mediterranean, in general, and Ionian Basin in particular cannot be resolved from classical kinematic constraints such as magnetic isochrones. Different reasons are advocated. Most of the deep basins have been consumed in the Hellenic and Calabrian subduction zones (Rosenbaum et al., 2004; Speranza et al., 2012), oceanic crust may have been formed during the Cretaceous quiet zone, or basins may have been short-lived, narrow, and thus atypical. Jurassic to present-day reconstructions are mainly based on global plate kinematics constrained by paleomagnetism, two of the key elements being the relative motion of Africa with respect to Eurasia and the position of the Adriatic block. Adria and Africa paleomagnetic poles seem to coincide as early as Permian time, with only small fluctuations since then (e.g., Channell, 1992; Muttoni et al., 1996, 2003, 2013; Rosenbaum et al., 2004, and references therein), suggesting no significant rotation of Apulia with respect to Africa during the opening of the Ionian Basin (Rosenbaum et al., 2004). Recent studies suggest small amounts of post-20-Ma rotation (Le Breton et al., 2017; Van Hinsbergen et al., 2014) perhaps responsible for some of the Ionian Basin Miocene deformation (Chamot-Rooke, Rangin, et al., 2005; Gallais et al., 2011), although a coherent tectonic link has not been established so far. The maximum width of the Ionian Basin inferred from most paleogeographic restorations (e.g., Barrier et al., 2008; Catalano et al., 2001; Dercourt et al., 1993; Frizon de Lamotte et al., 2011; Rosenbaum et al., 2004) is far below the potential detection of paleomagnetic methods. Therefore, constraints on the evolution of the East Mediterranean mainly rely on geological constraints from the different subbasins.

Permian marine basins are found along most of the margins of the eastern Mediterranean (Frizon de Lamotte et al., 2013; Guiraud et al., 2005; Stampfli et al., 2001), for example, in northern Syria (Palmyra through; e.g., Garfunkel, 1998), southern Tunisia (Jeffara Basin, synthesis in Mejri et al., 2006), western central Sicily (Sicanian and Imerese successions; Basilone, Frixa, et al., 2016; Catalano et al., 1991), and eastern Crete (Robertson, 2006). The interpretation of these basins either as remnants of oceanic pelagic sequences or as rift basins preceding oceanic spreading provides the main argument for geodynamic scenarios favoring an Early to Middle Permian age (Figure 2; e.g., Ben-Avraham & Ginzburg, 1990; Catalano et al., 1991; Vai, 2003) or Late Permian to Early Triassic age for the East Mediterranean Basins (Stampfli et al., 1991, 2001; Stampfli & Borel, 2002). However, across North Africa, little evidence for syntectonic faulting is found, and clear links between these Permian rifts and the offshore deep Mediterranean basinal domain are missing (Frizon de Lamotte et al., 2013; Garfunkel, 1998; Raulin et al., 2011). Alternatively, Permian sequences are described as a passive sagging phase sealing a Late Devonian-Early Carboniferous extensional event (Frizon de Lamotte et al., 2013).

Fault activity is imprinted in Middle to Upper Triassic (late Anisian to Norian) sediments along the Levant margin (e.g., Gardosh & Druckman, 2006; Garfunkel, 1998; Garfunkel & Derin, 1984). To the west, deep water pelagic sediments are deposited from early Ladinian onward in the Lagonegro Basin (Ciarapica & Passeri, 2002). Deformed remnants of this basin are presently integrated as part of allochthonous thrust sheets in the Apennines (Figure 1; Scrocca, 2010, and references therein). Following Catalano et al. (2001), the Lagonegro succession was likely deposited over a moderately stretched continental crust (20–30 km thick) and is therefore unlikely to represent the direct equivalent of the deep sedimentary sequences of the Ionian Basin. The precise restoration of the Lagonegro sequences and its relation with the Ionian Basin in Middle Triassic remains a matter of debate. The Lagonegro Basin may have been connected to the Pindos Basin (Robertson, 2006), or it may be a failed propagation of the Neo-Tethys ocean toward the Ionian Basin (Şengör et al., 1984). Based on magnetic modeling, Speranza et al. (2012) suggest a Carnian age for oceanic spreading in the Ionian Basin (Figure 2), interpreting the Lagonegro succession as deposited on the adjacent rifted domain. Rosenbaum et al. (2004) acknowledge that oceanic spreading

in the Ionian Basin might have occurred as early as the Triassic but was more likely limited to the Jurassic (Figure 2).

The main rifting phase related to the formation of the Levant margin occurred from latest Triassic to early Middle Jurassic time (Gardosh et al., 2010; Gardosh & Druckman, 2006; Garfunkel, 1998, 2004). The architecture of the Levant and Egyptian margins and the orientation of the Eratosthenes seamount (approximately NE-SW, Figure 1) and transform faults (Figure 1; Montadert et al., 2014; Tassy et al., 2015) support a NW-SE direction of extension (e.g., Barrier et al., 2008; Chamot-Rooke, Rangin, et al., 2005; Frizon de Lamotte et al., 2011; Gardosh et al., 2010; Gardosh & Druckman, 2006; Garfunkel, 1998, 2004; Garfunkel & Derin, 1984; Tari et al., 2012). Evidence for rifting over the same period is also reported in Libya (Arsenikos et al., 2013), Tunisia (Raulin et al., 2011), and Sicily (Basilone et al., 2010; Basilone, Sulli et al., 2016). Syntectonic basaltic flows are observed in the Levant margin (early Lower Jurassic Asher volcanics; Garfunkel & Derin, 1984) and onshore and offshore Sicily (e.g., early Middle Jurassic; Basilone et al., 2010; Patacca et al., 1979; Yellin-Dror et al., 1997). Based on these observations, most paleogeographic models suggest a synchronous onset of opening/spreading in the Herodotus and Ionian Basins in Toarcian to early Bajocian time (e.g., Barrier et al., 2008; Frizon de Lamotte et al., 2011; Garfunkel, 1998, 2004). In contrast, Robertson (2007) suggests a diachronous continental breakup between the Herodotus (Early Jurassic) and Ionian basins (Late Jurassic). The termination of oceanic spreading is inferred to occur either in the Tithonian (Barrier et al., 2008; Frizon de Lamotte et al., 2011), Early Cretaceous (Garfunkel, 1998, 2004), or Late Cretaceous to Early Tertiary time (Catalano et al., 2001; Figure 2).

From latest Jurassic to early Late Cretaceous, a renewed episode of extension is evidenced across the proximal domains of the North African margin in Lebanon (Homberg et al., 2010), the Western Desert (Moustafa, 2008), Cyrenaica (Arsenikos et al., 2013), and the Chott Basin in Tunisia (Gabtni et al., 2013). Volcanic activity is also reported locally (e.g., see syntheses in Dercourt et al., 1986, and Garfunkel, 1998). Several geodynamic models rely on these observations to suggest a Cretaceous continental breakup in the Ionian and Herodotus Basins (Dercourt et al., 1986, 1993; solution retained in Chamot-Rooke, Rangin, et al., 2005).

The onset of convergence between Africa and Europe by the Late Cretaceous was accommodated by discontinuous reactivation and inversion episodes (e.g., Frizon de Lamotte et al., 2011; Jolivet et al., 2015; Roure et al., 2012, and references therein) that did not totally obliterate earlier rift episodes (Figure 1). Discrete steps of the inversion (Santonian and Middle-Late Eocene) are recorded on the Cyrenaica margin of the Ionian Basin (Arsenikos et al., 2013). They are interpreted as transient events triggered by far-field forces that originated at the Hellenic subduction zone (Arsenikos et al., 2013).

Neogene intra-Ionian Basin compression is now well documented as a complex network of NE trending reverse faults in the prolongation of the Medina mounts (Figures 1 and 3) and is interpreted as reactivation of a Mesozoic spreading fabric (Gallais et al., 2011; Le Meur, 1997; Pagot et al., 1999; Sioni, 1996). The timing of inversion is restricted to latest Miocene (Tortonian) in relation with a plate reorganization preceding the main phase of opening of the Tyrrhenian Basin (Chamot-Rooke, Rangin, et al., 2005; Gallais et al., 2011), and probably not Late Cretaceous to Paleogene as suggested by Roure et al. (2012). The same structures were interpreted as Late Miocene tilted blocks evidencing extension of the African plate (e.g., Hieke et al., 2003, 2009), suggesting very recent formation of the basin (Fabricius & Hieke, 1977; Fabricius, 1984; Figure 2).

2.2. Present-Day Structure and Previous Interpretations

Part of the Ionian Basin has been subducted beneath Calabria in the wake of the opening of the Liguro-Provençal and Tyrrhenian basins (Chamot-Rooke et al., 1999; Faccenna et al., 2003; Malinverno & Ryan, 1986), while the northern portion of the basin (of unknown size) has been consumed beneath the Hellenic Arc (Biju-Duval et al., 1978). The Ionian crust and Mesozoic series are largely draped by two young accretionary wedges: the Calabrian prism and the Mediterranean Ridge (Biju-Duval et al., 1978; Ryan et al., 1982; Figures 1 and 3), the former being contemporaneous with the late Miocene/Pliocene opening of the Tyrrhenian, and the latter with the Miocene rollback of the Hellenic trench (Jolivet et al., 2008; Jolivet & Brun, 2010). Both accretionary wedges are segmented and show lateral variations in their structural style

10.1029/2018TC005472

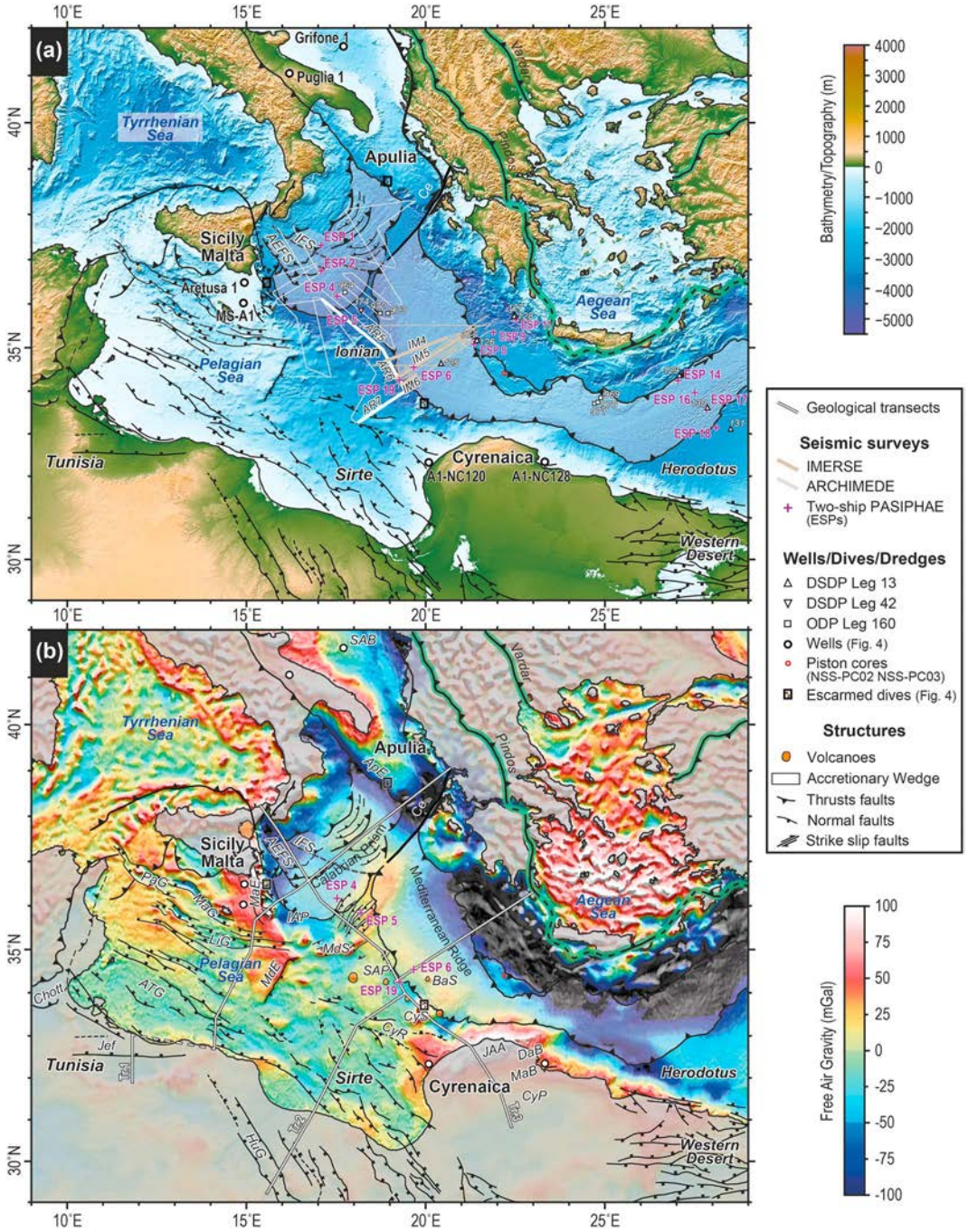

Figure 3. (a) Bathymetric map showing the location of the data sets used in this study (bathymetric grid from Becker et al., 2009). Reprocessed sections from the ARCHIMEDE and IMERSE reflection seismic surveys shown in this study are indicated by thicker lines: AR5 and AR6 (Figure 10), AR7 (Figure 7) and IM 5 (Figure 9), and IM4 and IM6 (Figure 11). (b) Free-air gravity map (Sandwell et al., 2014) overlain by the horizontal gradient showing the main morphostructural features of the study area. AEFA: Alfeo-Etna Fault system; ApE: Apulia Escarpment; ATG: Ashtart-Tripolitania Graben; BaS: Bannock Seamount; Ce: Cephalonia Fault; CyR: Cyrenaica Ridge; CyP: Cyrenaica Platform; CyS: Cyrene Seamount; DaB: Darnah Basin; HuG: Hun Graben; IAP: Ionian Abyssal Plain; IFS: Ionian Fault System; JAA: Jabal Al Akhdar; Jef: Jeffara Basin; LiG: Linosa Graben; MaB: Mamarica Basin; MaE: Malta Escarpment; MaG: Malta Graben; MdE: Medina Escarpment; MdS: Medina Seamount; PaG: Pantellaria Graben; SAB: South Adriatic Basin; SAP: Sirte Abyssal Plain (after Arsenikos et al., 2013; Chamot-Rooke, Rangin, et al., 2005; Frizon de Lamotte et al., 2011; Gallais et al., 2011; Polonia et al., 2011, 2016, 2017; Robertson, 2007, and own observations).

(e.g., Chaumillon & Mascle, 1995, 1997; Minelli & Faccenna, 2010; Polonia et al., 2016) dependent upon convergence parameters, the nature and depth of the décollement levels, and the structure of the subducting plate and backstop (e.g., Bortoluzzi et al., 2017; Chaumillon et al., 1996; Gutscher et al., 2017; Reston, Fruehn, et al., 2002; Reston, Von Huene, et al., 2002). To the south, the structure of the African margin of the Ionian Basin is complex and may be delimited by the Eastern Sicily/Malta and Cyrenaica segments, with the offshore Sirte Basin in between. To the north, the Apulian conjugate margin is partially preserved where it was not subducted, that is, west of the Cephalonia strike-slip fault (Figure 1).

The Ionian Basin is floored with thin crust (less than 8–10 km thick) according to refraction data and/or gravity inversions (Cowie & Kusznir, 2012; de Voogd et al., 1992; Dellong et al., 2018; Ferruci et al., 1991; Hinz, 1974; Makris et al., 1986; Nicolich et al., 2000), comparable to the crust of the Herodotus and Levant basins farther east (e.g., Ben-Avraham et al., 2002; Makris et al., 1983; Netzeband et al., 2006; Steinberg et al., 2018). In all three basins (Ionian, Herodotus, and Levant), the nature of the crust is still a matter of debate. Oceanic crust is favored in the Ionian Basin (e.g., Catalano et al., 2001; Chamot-Rooke, Rangin, et al., 2005; Dannowski et al., 2019; de Voogd et al., 1992; Dellong et al., 2018; Makris et al., 1986; Speranza et al., 2012). Alternative hypotheses include thin continental crust (e.g., Finetti, 1982; Hieke et al., 1998, 2003, 2009; Roure et al., 2012) or exhumed mantle based on analogies with observations made at present-day magma-poor ocean-continent transitions (Sioni, 1996).

Overlying this thin crust, sedimentary sequences up to 10 km thick have been identified (e.g., Chamot-Rooke, Rangin, et al., 2005; Finetti, 1982; Finetti & Del Ben, 2005; Finetti & Morelli, 1972; Gallais et al., 2011; Minelli & Faccenna, 2010; Polonia et al., 2011; Sioni, 1996). Some of the shallowest successions have been correlated laterally, such as the Messinian evaporites, but attempts to correlate the deepest sequences at the scale of the entire basin are scarce and somewhat inconsistent (Finetti, 1982; Finetti, 2005; Finetti & Morelli, 1972). The scarcity of available data pertinent to the deep Ionian Basin sequences explains the large uncertainties (Figure 2) regarding the timing and orientation of the rifting phase(s), lithosphere thinning, and oceanic spreading (if any). Calibrating the deepest sequences of the adjacent margins (Apulia, Eastern Sicily/Malta, and Cyrenaica) is clearly necessary to reach a consistent tectonostratigraphic framework.

3. Data Set Review and Seismic Reflection Processing

3.1. Reflection Seismic Data: Acquisition Parameters and Processing

Few seismic lines show deep sedimentary sequences in the Ionian Basin with a reasonable resolution. IMERSE (1994) and ARCHIMEDE (1997) surveys were designed for deep investigation and consequently show widespread reflectors as deep as 9–10 s (twtt; e.g., Chamot-Rooke, Rangin, et al., 2005; Gallais et al., 2011, 2012, 2013; Le Meur, 1997; Pascal, 1997; Reston, Fruehn, et al., 2002; Reston, Von Huene, et al., 2002; Sioni, 1996). Lines that showed clear lateral variations of the deepest sequences were selected and reprocessed using the CGG Geocluster® software.

In 1997, 2,500 km of multichannel seismic reflection data were collected over the Ionian and Sirte abyssal plains, Calabrian prism, and Medina Seamounts during the ARCHIMEDE cruise on board the R/V *Le Nadir* (Pascal, 1997; see Table S1 in the supporting information for detailed acquisition parameters). Standard processing of ARCHIMEDE profiles 5, 6, and 7 were carried out (Figure 3a). After a spectral analysis of the traces and a resampling at 8 ms, we applied band-pass and frequency-wave number (F, k) domain filtering and an external mute. Two successive velocity analyses were performed every 200 Common Depth Points to constrain lateral velocity variations. Prestack spherical divergence correction and deconvolution were applied. After stack, a constant-velocity frequency-wave number (F, k) time migration was applied combined with random noise attenuation, gain reinforcement, and dynamic amplitude equalization. We applied an antimultiple on the ARCHIMEDE 6 profile based on the Delft Surface Multiple Attenuation model and SRME Surface multiple elimination of (Berkhout & Verschuur, 1997).

In 1994, over 2,500 km of multichannel seismic reflection data were collected over the Mediterranean Ridge during the IMERSE survey on board the R/V *Explora* (see Table S1 for detailed acquisition parameters). A standard processing sequence was initially carried out (Le Meur, 1997; Reston, Fruehn, et al., 2002; Reston, Von Huene, et al., 2002). Poststack time migration using a constant velocity of 1,500 m/s was

reperformed for the IMERSE lines 4, 5, and 6 (Figure 3a). In addition, four O.B.H. stations were deployed during the course of the survey over the internal part of the Mediterranean prism and recorded refracted and wide-angle arrivals (Jones et al., 2002).

3.2. Refraction Seismic

Several refraction seismic experiments of different resolution were conducted in the Ionian Basin (Dellong et al., 2018; Ferruci et al., 1991; Hinz, 1974; Makris et al., 1986; Nicolich et al., 2000). The most recent and highest-resolution constraints on the crustal structure of the western Ionian Basin and Malta escarpment come from the DIONYSUS wide-angle seismic survey (Dannowski et al., 2019; Dellong et al., 2018). The velocity information obtained was used to constrain geological transects at depth (location Figure 3b).

The two-ship Expanding Spread Profile (ESPs of the PASIPHAE cruise) were shot in 1988 (see Table S1 for acquisition parameters), focusing on three transects (Figure 3a; Lallemant et al., 1994; Truffert et al., 1993; de Voogd et al., 1992): the Calabrian prism (ESPs 1, 2, 4, and 5), the Western Mediterranean Ridge (ESPs 19, 6, 8, 9, and 11), and the eastern Mediterranean Ridge (ESPs 18, 17, 16, and 14). Correlations with seismic reflection profiles of ESPs 4, 5, 6, and 19 by Le Meur (1997) provided first-order information on the velocity structure of the Ionian Basin sedimentary sequences and basement. ESPs are the only available deep constraint in the eastern part of the Ionian Basin (toward the Sirte Abyssal Plain) and were helpful to reach a consistent seismic stratigraphy.

3.3. Well Data, Piston Core, Dredges, and Dives

The Deep Sea Drilling Project (DSDP) and Ocean Drilling Program (ODP) represent the only direct access to the sedimentary sequences of the Ionian Basin (Figure 3a): DSDP Legs 13 (sites 125–131; Ryan & Hsu, 1973) and 42 (sites 377 and 374; Hsu & Montadert, 1978) and ODP Leg 160 (sites 964 and 969–973; Emeis et al., 1996). Except for DSDP site 374 located within the Ionian Abyssal Plain, other drillings are either located over the Calabrian and Mediterranean accretionary wedges or near the Hellenic trench. Since these drillings remained quite shallow, the major results mainly document the Neogene sedimentary history, while information on deeper successions and structures is missing. Piston cores in the Ionian and Sirte abyssal plains mainly bring information on Quaternary deposits (Hieke et al., 2003, 2009; Polonia et al., 2013). Indirect observations of deeper sedimentary sequences come from piston cores in mud volcanoes, acting as natural channels that transport deep material to the seafloor. Several mud volcano provinces are found over the Mediterranean Ridge (see synthesis in Kioka et al., 2015). Many of them concentrate near the tectonic contact between the accretionary prism and the Hellenic backstop (Chamot-Rooke, Rabaute, et al., 2005; Rabaute & Chamot-Rooke, 2007) where cores recovered mud breccia samples containing clasts of shale, siltstone, and limestone as old as Late Jurassic to Early Cretaceous (e.g., Kioka et al., 2015; Ryan et al., 1982). The origin of the mud and the expulsion mechanisms remain unclear, casting uncertainty on whether the clasts were derived from the subducting plate or from the backstop. Petrography and maturity analyses of the mud matrix and clasts performed by Kioka et al. (2015) suggest that at least some of the oldest clasts were likely detached from the subducting plate at the contact with the backstop, hence possibly representing an indirect window on sediments deposited in the Ionian Basin (Figure 3).

Numerous wells document the stratigraphic evolution of the Ionian Basin margins. We selected several relevant ones (Figures 3 and 4) that document the age of platform-basin transition along different segments of the Ionian margins (Apulia, Eastern Sicily/Malta, and Cyrenaica). We used the Visibility of Petroleum Exploration Data in Italy public domain database for the Grifone 1, Puglia 1, and Aretusa 1 wells (ViDEPI project) and published wells MS-A1 (Jongsma et al., 1985), A1-NC120, and A1-NC128 (Arsenikos, 2014; Duronio et al., 1991; Yanilmaz et al., 2008). Dredges and dives performed (Figure 4) along the Apulia and Malta escarpments and along the slopes of the Cyrene, Medina, and Alfeo seamounts (Biju-Duval et al., 1982; Charier et al., 1987, 1988; Groupe-Escarmed et al., 1987; Rossi & Borsetti, 1977; Scandone et al., 1981) provide a unique record of the rocks that form the present-day escarpments, enabling us to present tentative age correlations of the deep sedimentary sequences of the Ionian Basin.

4. Tectonostratigraphic Evolution of the Ionian Basin Margins

The passive margins delimiting the Ionian Basin can be divided into different segments: (1) the Apulian, (2) Eastern Sicily/Malta, (3) Sirte, and (4) Cyrenaica segments (Figure 3).

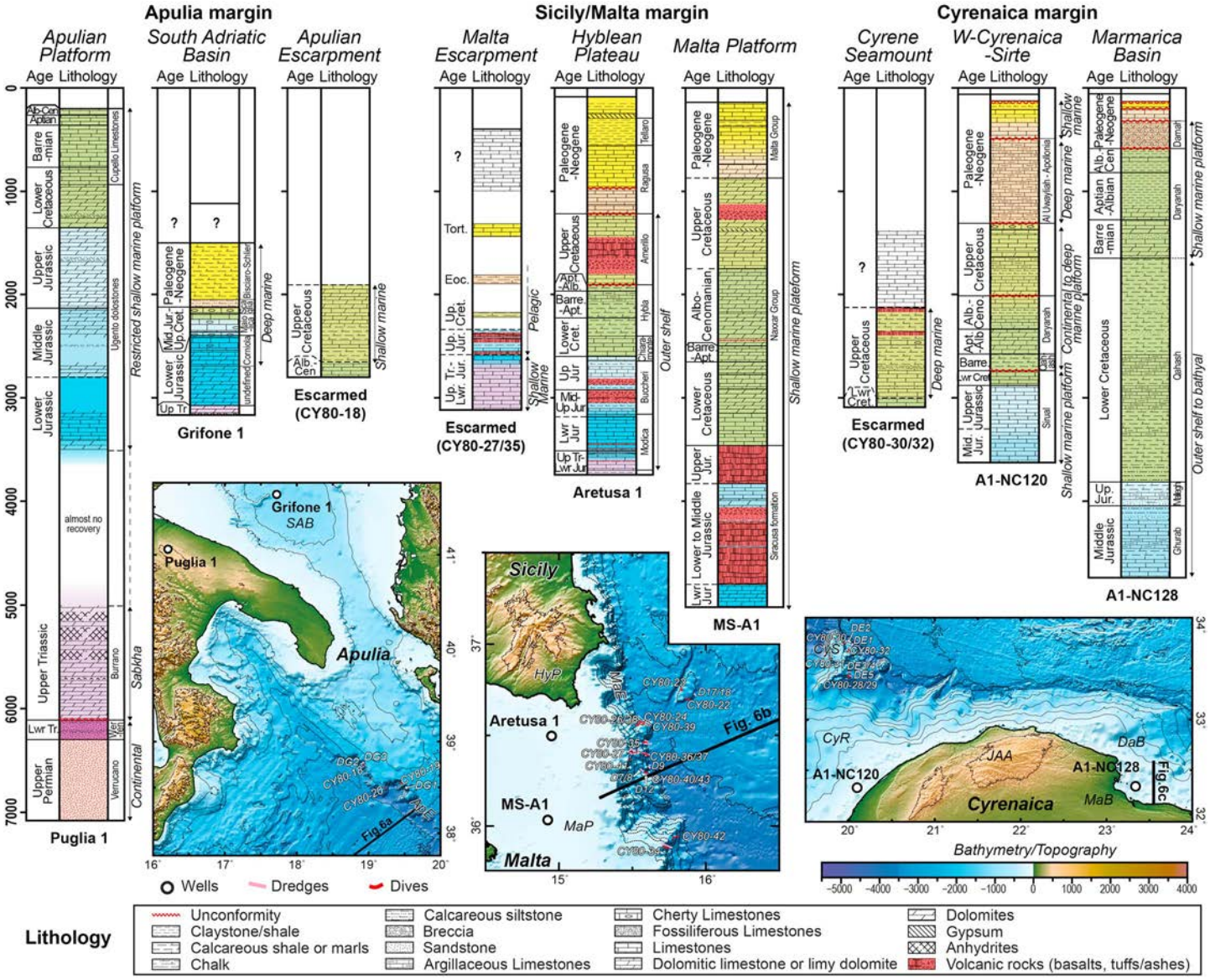

Figure 4. Lithology, age, and thicknesses of selected wells and dives located within the platforms and along the escarpments surrounding the Ionian Basin (location on insert maps). (1) Apulia margin: Grifone 1 and Puglia 1 (from the ViDEPI Project—http://unmig.sviluppoeconomico.gov.it), Escarmed dive CY80-18 (from Charier et al., 1988). (2) Sicily/Malta margin: Aretusa 1 and MS-A1 (respectively from the VIDEPI Project, n.d.and after Jongsma et al., 1985), Escarmed dive CY80-27/35, (after Biju-Duval et al., 1982). (3) Cyrenaica margin A1-NC120 and A1-NC128 (compiled from Arsenikos, 2014; Duronio et al., 1991; Yanilmaz et al., 2008), Escarmed dives CY80-30/32 (after Groupe-Escarmed et al., 1987). ApE: Apulian Escarpment; CyS: Cyrene Seamount; CyR: Cyrenaica Ridge; DaB: Darnah Basin; HyP: Hyblean Plateau; JAA: Jabal Al Akhdar; MaB: Marmarica Basin; MaE: Malta Escarpment; MaP: Malta Platform; SAB: South Adriatic Basin.

4.1. Apulian Segment

The Apulian margin segment exposed at the southwestern termination of the Adriatic plate (Figures 1 and 3) represents the only well-preserved portion of the conjugate North African passive margin west of the Cephalonia Fault (Finetti, 1982). The Apulian margin segment preserves a thick (up to 5-km thick) Mesozoic carbonate platform (Argnani, 2013; Finetti, 1982; Finetti & Del Ben, 2005; Santantonio et al., 2013; Vlahović et al., 2005) delimited from the Ionian Basin by a steep NW-SE oriented escarpment separated from the front of the Calabrian prism by a narrow corridor (Figures 3 and 4).

The oldest sediments recovered from drill holes within this segment (Figure 4) correspond to siliciclastic continental deposits attributed to the Permian and Lower Triassic based on facies correlations with the

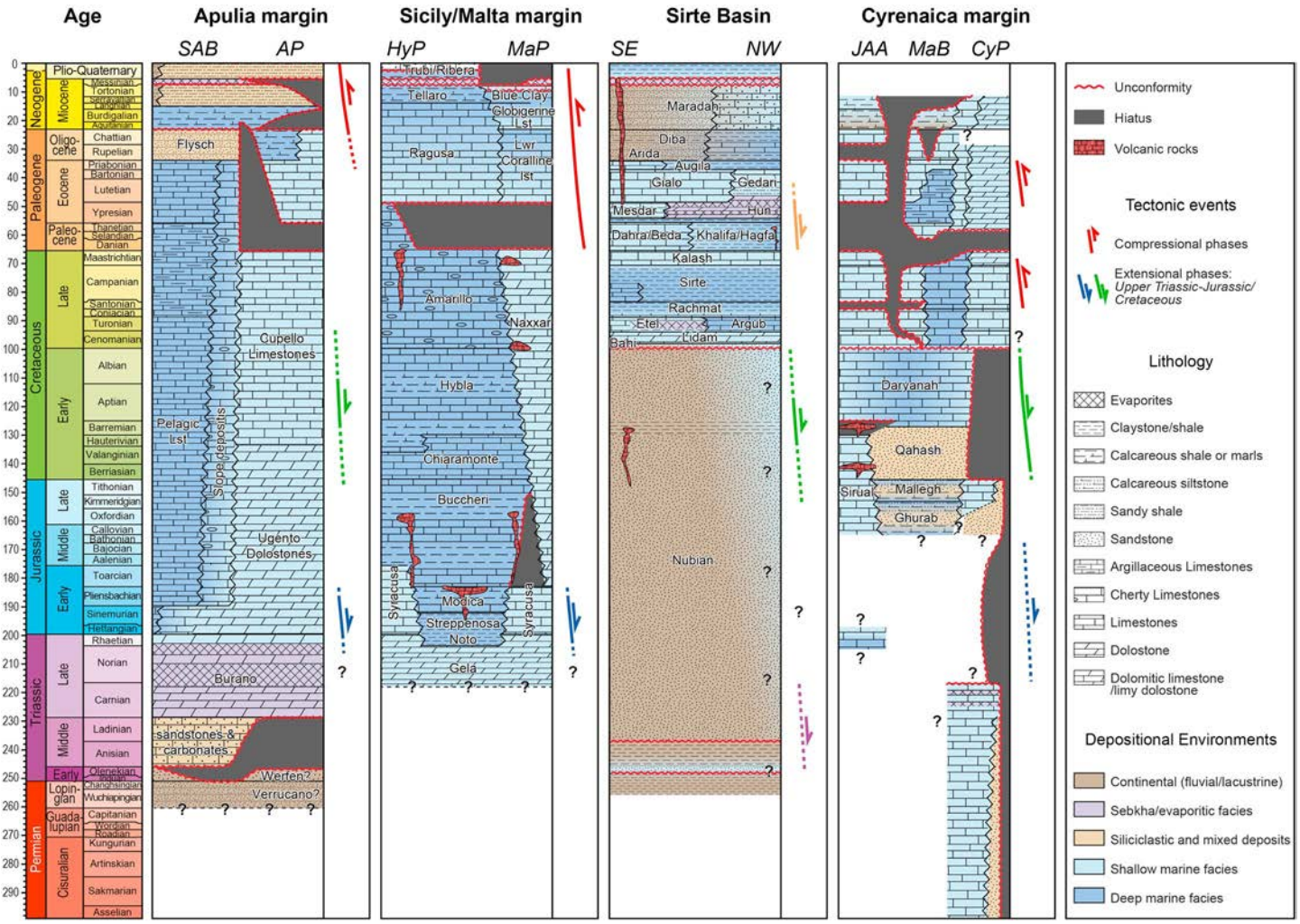

Figure 5. Tectonostratigraphic charts of Ionian Basin margins. (1) Apulia margin (based on Argnani, 2013, and Santantonio et al., 2013), (2) Sicily/Malta margin (compiled from Lipparini et al., 2009, and Yellin-Dror et al., 1997), (3) Sirte Basin (after Abadi et al., 2008; Wennekers et al., 1996), and (4) Cyrenaica margin (compiled from Arsenikos et al., 2013; Martin et al., 2008). Time scale from Gradstein and Ogg (2004). SAB: South Adriatic Basin; AP: Apulian Platform; HyP: Hyblean Platform; MaB: Mamarica Basin; MaP: Malta Platform; JAA: Jabal Al Akhdar; CyP: Cyrenaica Platform (location in Figure 1).

Verrucano and Werfen formations (Puglia 1, Figures 4 and 5; ViDEPI Project). Middle Triassic sandstones and carbonates locally overlie these formations above an angular unconformity (Figure 5; ViDEPI Project; Santantonio et al., 2013). The overlying Upper Triassic is characterized by evaporites and dolostone of the Burano Formation locally up to 1.8 km thick (Santantonio et al., 2013). The early Lower Jurassic (Hettangian-Sinemurian, possibly up to the Pliensbachian) records the progressive individualization of deeper basins within the Apulian platform (e.g., the south Adriatic basin) and within the Ionian zone farther east (Figures 3 and 4; Argnani, 2013; Del Ben et al., 2015; Santantonio et al., 2013; Vlahović et al., 2005). The formation of these basins is related to an ongoing rift event that possibly initiated earlier in the Triassic (Del Ben et al., 2015). Shallow marine conditions prevailed over the Apulian platform until Paleogene time. Minor extensional activity occurred once again in the Early Cretaceous (Del Ben et al., 2015; Santantonio et al., 2013). The transition from carbonates to siliciclastic sedimentation in Oligocene-Early Miocene time marks the involvement of the Apulian platform in the common foredeep of the Apennines and Dinarides orogenic system (Argnani, 2013). More generally, the same transition is observed everywhere around Africa and coincides with a major Mid-Oligocene sea level fall and a phase of tectonic inversion along the North African margin.

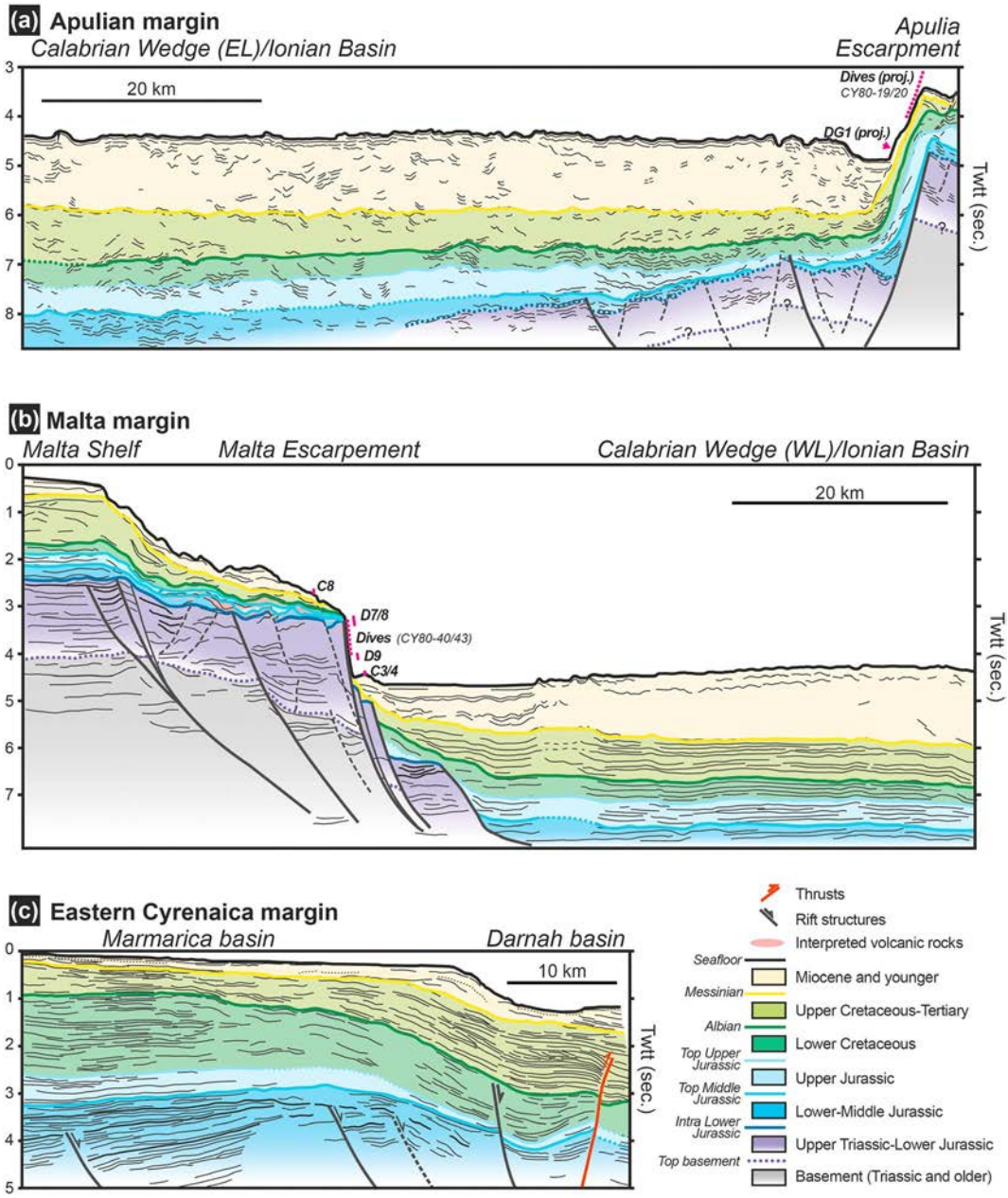

Figure 6. Interpretive line drawings across the Apulian (ARCHIMEDE 31, uninterpreted data available as Figure S1) and Malta escarpments (seismic profile from Minelli & Faccenna, 2010) and Cyrenaica platform (after Arsenikos, 2014; Arsenikos et al., 2013). Dredges, dives, and cores are projected from less than 5 km along Malta Escarpment and less than 40 km along the Apulian Escarpment. The well A1-NC128 that enabled stratigraphic calibrations over eastern Cyrenaica (Arsenikos et al., 2013) is projected at a distance of less than 20 km. The location of the profiles, dredges, and dives projected is shown in Figure 4. EL: Eastern Lobe; WL: Western Lobe (as defined in Polonia et al., 2011, 2016, see Figure 3).

We use these constraints to interpret the ARCHIMEDE 31 profile, which crosses the scarp at the edge of the Apulian platform toward the Ionian basin (Figure 6). This transition is documented in several studies (Catalano et al., 2001; Del Ben et al., 2015; Finetti, 1982; Minelli & Faccenna, 2010) providing reasonable constraints over the Apulian platform despite the low quality of the profile. The sedimentary sequences of the Ionian Basin are observable discontinuously beneath the allochthonous Calabrian prism between ~6- and ~8.5-s twtt (Figure 6a). We projected observations derived from the closest dives and dredges collected along the upper part of the Apulian escarpment on the profile (Figures 4–6a). The oldest rocks recovered from dredges correspond to shallow marine platform facies of late Early Cretaceous (Albo-Cenomanian)

to Late Cretaceous (Figures 3 and 4; Biju-Duval et al., 1982; Charier et al., 1988; Rossi & Borsetti, 1977). The slope initially formed as a result of the latest Triassic to Early Lower Jurassic rifting event and was subsequently buried beneath younger shelf breaks (Figure 6a). We tentatively tied several sequences from the Apulian platform to the Ionian Basin. The shallowest sequence encompasses the sediments forming the eastern lobe of the Calabrian Prism (as defined in Polonia et al., 2011, 2016) corresponding to Messinian to present-day sediments. The underlying Miocene to Upper Cretaceous sequence is directly calibrated from the escarpment, while the Lower Cretaceous and notably the Upper Jurassic are correlated with greater uncertainties. The deepest reflectors (below 8-s twtt) might be of Early to Middle Jurassic age if interpreted as the first sediments resting directly over the Upper Triassic to Lower Jurassic sequence on the Apulian platform.

4.2. Eastern Sicily/Malta Segment

This segment of the Ionian Basin rifted margin follows the NNW-SSE oriented Malta scarp from east Sicily to the approximately E-W trending Medina Seamounts ridge (Figures 3 and 4). The Hyblean Plateau (SE Sicily) and Malta platforms bordering the escarpment preserve more than 5 km of Mesozoic to Neogene series (Patacca et al., 1979). Farther south, the Ionian margin runs along the edge of the Pelagian platform and basins (Frizon de Lamotte et al., 2011) marked by the Medina escarpment (Figures 1 and 3).

The oldest series recovered from the Hyblean Plateau and Malta platforms correspond to Upper Triassic shallow marine dolomitic limestones and bioclastic carbonates of the Gela Formation (Figures 4 and 5), also including evaporites laterally (Nafta Formation; Patacca et al., 1979). The onset of rifting during the latest Triassic (Rhaetian) is recorded by the progressive individualization of deeper basins (e.g., Streppenosa Basin in the Hyblean Plateau; see Casero & Roure, 1994), where interbedded dolomitic limestones and basinal black shales of the Noto and Streppenosa formations were successively deposited (Patacca et al., 1979; Yellin-Dror et al., 1997). Shallow marine conditions persisted during Early Jurassic time over the Hyblean and Malta platforms with the deposition of limestones of the Syracusa Formation, whereas marls and marly limestones of the Modica Formation are recorded in the basin (Patacca et al., 1979). Basalts and hyaloclastites are reported within these sequences in several wells of the area (Figures 4 and 5; Jongsma et al., 1985; Patacca et al., 1979). Deepening of the Malta Escarpment initiated in middle to late Early Jurassic time, recorded by a change from shallow marine to basinal sequences (Bizon et al., 1985) associated with the occurrence of basalts and volcanoclastic material (Biju-Duval et al., 1982; Charier et al., 1987). Local volcanic activity persisted during the deposition of marls and marly and cherty limestones of the Buccheri Formation from Middle to Late Jurassic time (Patacca et al., 1979; Yellin-Dror et al., 1997). Pelagic conditions prevailed over the Hyblean plateau during the Cretaceous up to middle Eocene with the deposition of cherty limestones and marls (Chiaramonte, Hybla, and Amerillo Formations (Figures 4 and 5; Patacca et al., 1979; Yellin-Dror et al., 1997). Concurrently, shallow marine dolomitic limestones (Naxxar Formation) were deposited over the Malta platform (Figures 4 and 5; Lipparini et al., 2009). Upper Cretaceous volcanic activity has been reported over the Hyblean Plateau and Malta platform (Figures 4 and 5; Yellin-Dror et al., 1997) and possibly along the scarp itself (Biju-Duval et al., 1982). From late Oligocene to Miocene time, pelagic limestone and marls were deposited over most of the Hyblean Plateau and Malta platform and are locally overlain by Messinian evaporites (Lipparini et al., 2009; Yellin-Dror et al., 1997).

We use the same reflection seismic profile as the one shown by Minelli and Faccenna (2010) to interpret the transition from the Malta shelf to the Ionian Abyssal Plain (Figure 6b). The numerous wells available over the Hyblean platform and Malta shelf (see ViDEPI database and selection in Figure 4) provide robust calibrations of sedimentary sequences as old as Upper Triassic (Casero & Roure, 1994; Yellin-Dror et al., 1997), even if the base is not constrained. Dives, dredges, and cores made along the Malta Escarpment document a large part of the offshore geology (Figure 4; Biju-Duval et al., 1982; Bizon et al., 1985; Charier et al., 1987; Enay et al., 1982; Scandone et al., 1981). We used and projected the closest and most relevant ones to interpret the profile (Figure 6b). The analysis of samples collected along the Malta escarpment documents the presence of Late Triassic-Early Jurassic shallow marine rocks forming the base of the scarp (Figure 4; Bizon et al., 1985; Charier et al., 1987; Scandone et al., 1981). These sequences are overlain by Middle to Late Jurassic pillow lavas and Upper Jurassic (Tithonian to Oxfordian) basinal marls (Bizon et al., 1985; Enay et al., 1982) cropping out along a smoother portion of the slope (Biju-Duval et al., 1982; Charier et al., 1987). The transition from the Malta Shelf to the Ionian Basin across the Malta Escarpment is abrupt

and occurs over ~30-km distance, only accommodated by a few normal faults sealed by Lower Jurassic sequences (Figure 6b). Upper Triassic to early Lower Jurassic sequences seem to terminate abruptly at the toe of the escarpment and are progressively onlapped by the deep reflective sequences from the Ionian Basin. We present a tentative correlation of the sequences calibrated over the Malta shelf and escarpment toward the Ionian Basin (Figure 6b). The Messinian erosional surface over the Malta shelf is correlated to the basal décollement of the western lobe of the Calabrian Prism (defined in Polonia et al., 2011, 2016), defining the base of the youngest sequence. At the toe of the escarpment, the Miocene to Upper Cretaceous sequence is defined by a basal onlap surface delimiting the top of the underlying Lower Cretaceous sediments. Both Lower Cretaceous and Upper Jurassic sequences appear quite reflective. The top of the deepest sequence deposited in the Ionian Basin is characterized by series of toplaps. This sequence is supposed to comprise late Early Jurassic to Middle Jurassic sediments. It is the basinal age equivalent of the sediments that records a change in the depositional environment over the Malta escarpment (Figures 3 and 4). Its base is not imaged along this profile, but the top basement could be as deep as 9- to 10-s twtt (Polonia et al., 2017). Evidence for volcanic activity is widespread along the Malta escarpment and platform (Figure 5), suggesting that some of the deep sequences imaged could include a large portion of volcanoclastic material.

4.3. Sirte Segment

The Sirte segment runs from the Medina Escarpment and Seamounts in the west to the Cyrenaica platform in the east (Figure 3). Onshore, the Sirte Basin is characterized by a series of horst and grabens that extend offshore in the Gulf of Sirte (Figure 3; Anketell, 1996; Del Ben & Finetti, 1991; Finetti, 1982; Jongsma et al., 1985). The boundary between the offshore extension of the Sirte Basin and the Ionian Basin is marked by an elongated relative structural high, referred to as the Cyrenaica Ridge (Figures 3 and 7). This high merges to the east with the Cyrenaica segment (Arsenikos, 2014; Arsenikos et al., 2013; Del Ben & Finetti, 1991; Wennekers et al., 1996) and can be interpreted discontinuously to the west toward the Medina Escarpment and Seamounts in the free-air gravity map (Figure 3).

Knowledge of the Sirte Basin stratigraphy, structure, and evolution mainly relies on field observations and onshore well data (Abadi et al., 2008; Abdunaser, 2015; Abdunaser & McCaffrey, 2014; Wennekers et al., 1996), where crustal thinning was less severe than offshore (Cowie & Kusznir, 2012). As a result, the first-order architecture and infilling history of the offshore Sirte Basin is poorly constrained, notably prior to the Upper Cretaceous (Figures 5 and 7). Several studies suggest that the Sirte Basin formed at the location of a former basement high, that is, the Paleozoic Arch, which separates the Cyrenaica platform from the Ghadames Basin (Figure 1) farther west (Abdunaser & McCaffrey, 2015; Frizon de Lamotte et al., 2013; Massa & Delort, 1984; Wennekers et al., 1996). Most studies propose that the Sirte Basin underwent several phases of extension. However, in detail, a variable subsidence history seems to be recorded in the different subbasins (Abadi et al., 2008; Abdunaser & McCaffrey, 2015). A Middle to Upper Triassic extensional event is suggested, but its lateral extension and impact on the crustal architecture are poorly constrained (Del Ben & Finetti, 1991; Massa & Delort, 1984; Thusu, 1996; Wennekers et al., 1996). The main rift events that formed the Sirte Basin took place from latest Jurassic to Cretaceous time (Abadi et al., 2008; Abdunaser & McCaffrey, 2014; Anketell, 1996; Wennekers et al., 1996). An initial rift event occurred in Early Cretaceous time (Abadi et al., 2008; Anketell, 1996; Wennekers et al., 1996) corresponding to the deposition of continental to shallow marine clastic sediments (Figure 5; Bonnefous, 1972). The most important rift-related subsidence seems to occur in the early Late Cretaceous related to the deposition of thick marine sediments (Abadi et al., 2008) over a regional Cenomanian unconformity (AGOCO (Arab Golf Oil Company), 1980). In early Late Cretaceous time, a change in depositional environments is reported at the borders of this margin segment over the Cyrene and Medina seamounts (Figures 3 and 4; Biju-Duval et al., 1982; Charier et al., 1987; Groupe-Escarmed et al., 1987). A renewed episode of extension occurred in Paleocene to Early Eocene time (Abadi et al., 2008) related to the deposition of carbonates and evaporites (Figure 5). Tectonic activity still seems to occur in the Hun Graben and locally offshore (Capitanio et al., 2011).

The transition from the Sirte to Ionian Basin is illustrated by the ARCHIMEDE 7 profile (Figure 7). The section shows a clear structural and stratigraphic contrast between the two basins separated by the narrow Cyrenaica Ridge. Sequences younger than the Lower Cretaceous can be correlated confidently between the Sirte and Ionian Basin. The Cretaceous rift episode is documented by a series of faults delimiting tilted blocks mostly restricted to the Sirte Basin. Sequences older than Cretaceous cannot be ascertained within the Sirte

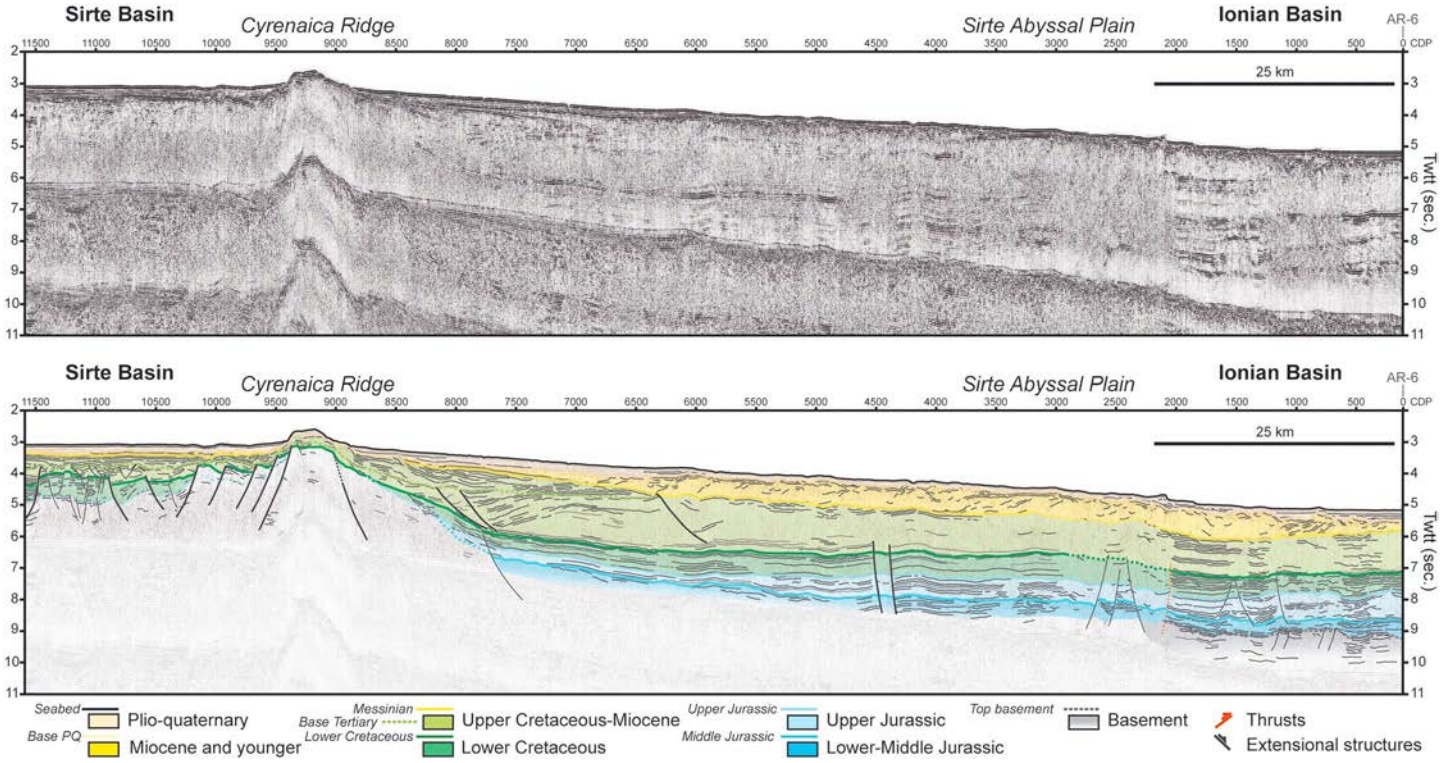

Figure 7. Interpretation of the ARCHIMEDE 7 seismic profile showing the transition from the Sirte to Ionian Basin across the Cyrenaica Ridge (location in Figure 3).

Basin, whereas deeper (and older) sequences appear quite clearly in the Ionian Basin. Ages of these deep sequences are based on correlations made at the scale of the whole Ionian Basin.

4.4. Cyrenaica Segment

The Cyrenaica promontory separates the Ionian and Sirte Basins to the west from the Western Desert area and Herodotus Basin to the east (Figures 1 and 3). The Mediterranean Ridge front directly borders the north Cyrenaica escarpment (Figure 3; Chaumillon & Mascle, 1995, 1997). A prominent ENE trending structural high—the Jabal Al Akdar Mountain—forms the northern part of the promontory north of a wide stable platform (Figures 1 and 3). The Jabal Al Akdar was formed by the Late Cretaceous and middle-late Eocene inversion of small rift basins (Arsenikos et al., 2013). Offshore to the northwest, the isolated Cyrene Seamount, which lies in the Sirte Abyssal Plain, is interpreted as the remnant of a horst-like structure (Biju-Duval et al., 1982; Groupe-Escarmed et al., 1987).

Results from several wells drilled onshore Cyrenaica document the stratigraphic evolution from Cambrian to Miocene time (Arsenikos et al., 2013; Keeley & Massoud, 1998; Martin et al., 2008; Yanilmaz et al., 2008). Triassic sequences in the wells of eastern Cyrenaica consist of coastal to shallow marine sandstones and mixed carbonates (Figure 5; Martin et al., 2008; Yanilmaz et al., 2008). The deposition of these sequences seems to have been controlled by NW-SE trending structures (Yanilmaz et al., 2008) pointing to Triassic extension over Cyrenaica (Keeley & Massoud, 1998). Regionally, the Early Jurassic time corresponds to a hiatus, whereas an acceleration of subsidence is recorded during the latest Early Jurassic in the previously formed rift basins (Keeley & Massoud, 1998). From Middle to Late Jurassic time, the southern part of Cyrenaica was emergent, while shallow marine conditions prevailed over a part of the Cyrenaica platform and the Jabal Al Akdar area (Yanilmaz et al., 2008) with the deposition of limestones of the Sirual Formation (Figures 4 and 5; Duronio et al., 1991). In contrast, north of the Cyrenaica platform (i.e., currently offshore), deep platform to basinal facies (argillaceous limestones, shales, sandstones, and siltstones) were deposited (Figures 4 and 5; Ghurab and Mallegh Formations; Duronio et al., 1991). The distribution of these sequences seems to follow a NW-SE trend until the Late Jurassic, until deposition became progressively

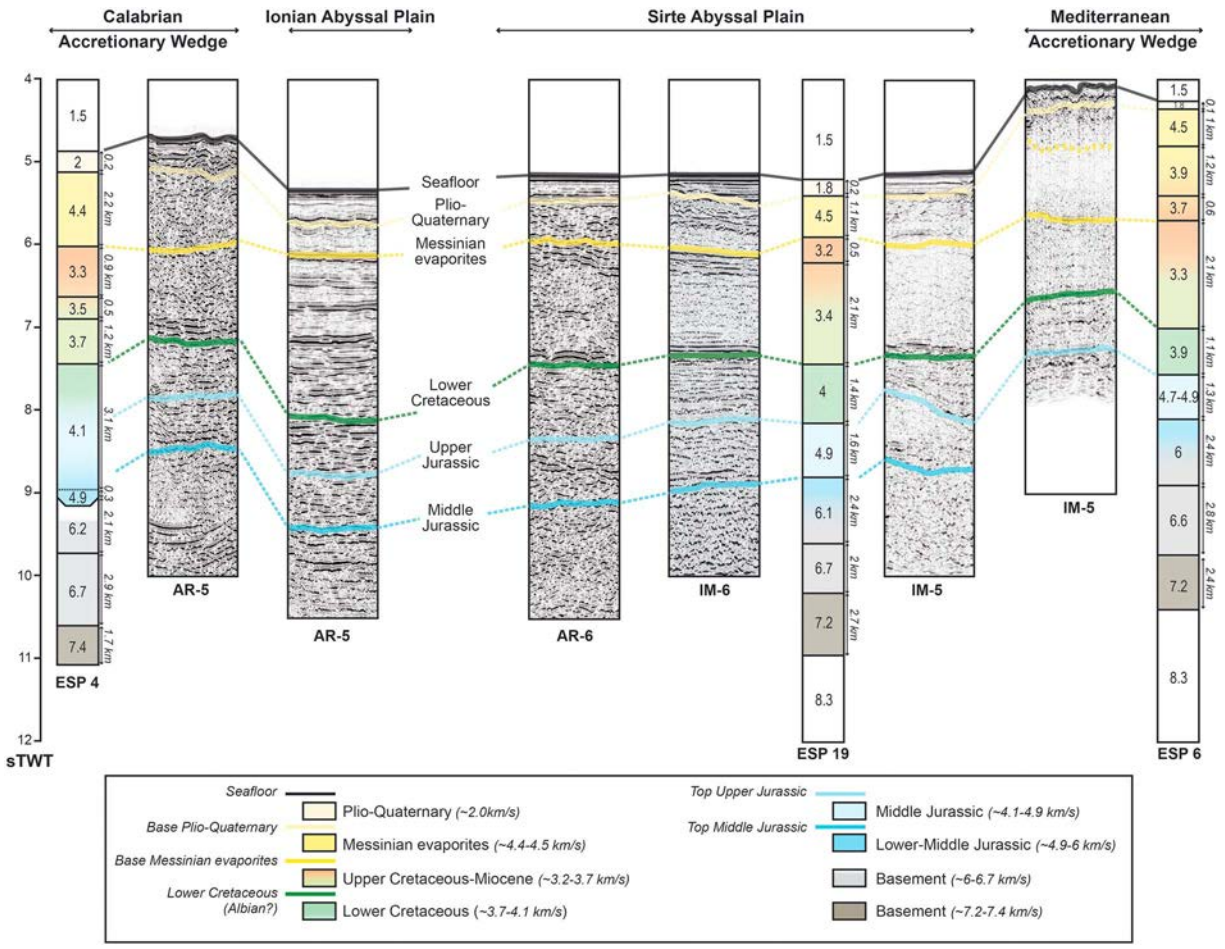

Figure 8. Seismic stratigraphy used in this work and age correlations suggested at the scale of the Ionian basin (Velocity models for the ESP 4, 19, and 6 are based on Le Meur, 1997). Seismic logs are extracted from the seismic profiles presented in this work close to the projected ESPs.

controlled by E-W trending structures (Arsenikos et al., 2013; Yanilmaz et al., 2008). This Early Cretaceous rift event is recorded over the northwestern part of Cyrenaica by a change from continental to basinal deposits (Figure 4, A1-NC120, Qahash and Daryanah Formations; Duronio et al., 1991), locally accompanied by volcanic rocks (Yanilmaz et al., 2008). A change in depositional environments (from shallow to deep marine) was also reported along the Cyrene Seamount in early Late Cretaceous time (Figures 3 and 4; Biju-Duval et al., 1982; Charier et al., 1987; Groupe-Escarmed et al., 1987). Two episodes of inversion are later recorded over Cyrenaica during Late Cretaceous and middle to late Eocene time separated by a period of relative tectonic quiescence during the Palaeocene (Arsenikos et al., 2013).

We were not able to correlate sedimentary sequences from the Cyrenaica segment toward the Ionian Abyssal Plain. Still, based on well calibrations over Cyrenaica (Arsenikos, 2014; Arsenikos et al., 2013), the two distinct rift events are evidenced in seismic profiles offshore Cyrenaica (Figure 6c). In addition to the well-documented Early Cretaceous rift, the occurrence of tilted block geometries sealed by Middle Jurassic sediments (Figure 6c) likely corresponds to the Triassic to Early Jurassic rift described onshore Cyrenaica (Arsenikos, 2014; Keeley & Massoud, 1998; Yanilmaz et al., 2008).

5. Seismic Stratigraphy and Correlations Across the Ionian Basin

The definition of seismic sequences across the Ionian Basin (Figure 8) relies on the regional correlation of seismic facies variations delimited by remarkable reflectors or unconformities, combined with *P* wave velocity information from the ESPs 19, 6, 4, and 5 (Le Meur, 1997). The age calibrations conducted along the escarpments (Figure 6) provide first-order age correlations between the Ionian and Sirte abyssal plains

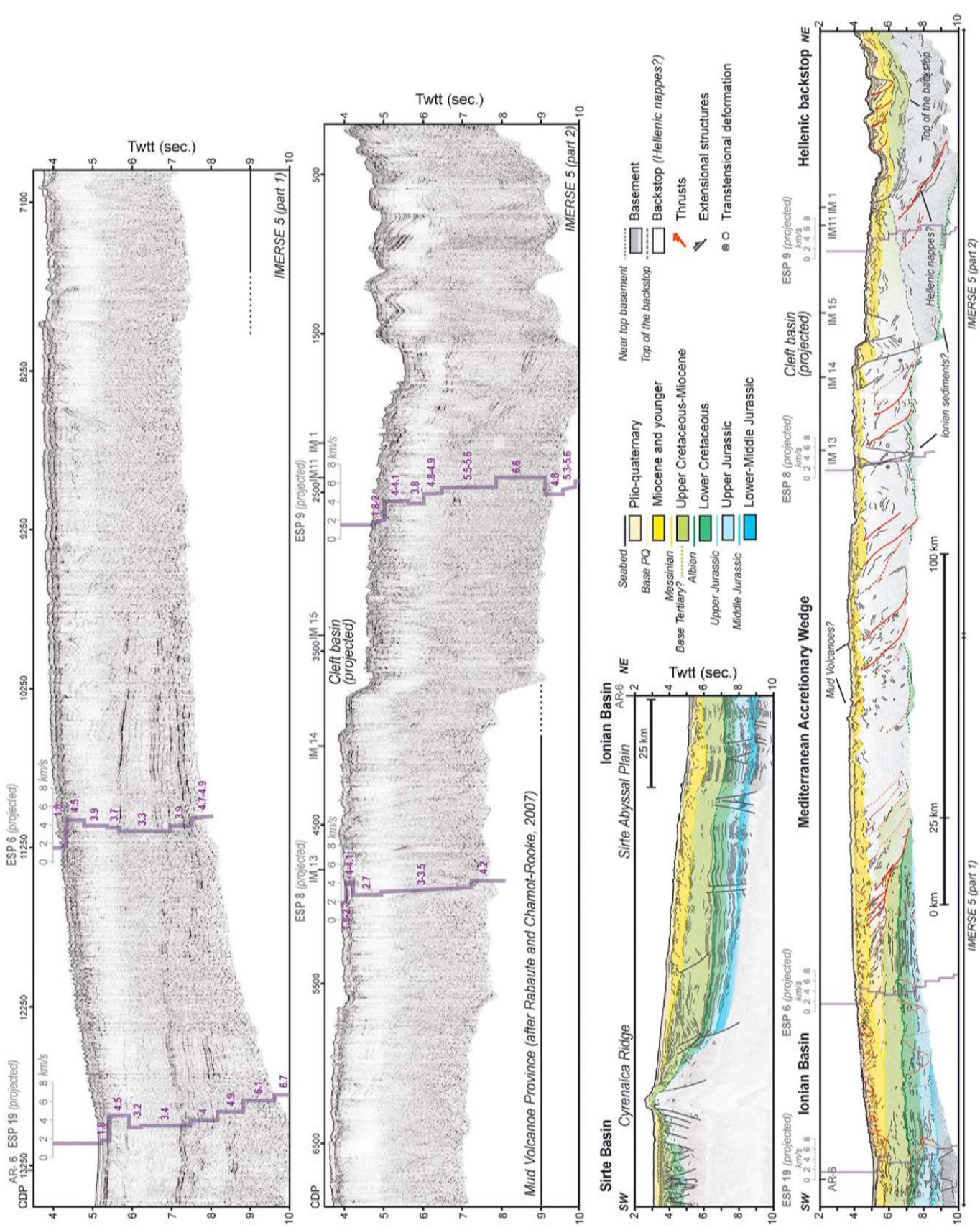

Figure 9. Interpretation of a SW-NE oriented seismic transect crossing the Ionian basin, the Mediterranean accretionary wedge, and the Hellenic backstop based on the ARCHIMEDE 7 and IMERSE 5 profiles (location Figure 3). ESPs 19, 6, 8, and 9 are from Le Meur (1997). Location of the Mud volcano province after Rabaute and Chamot-Rooke (2007).

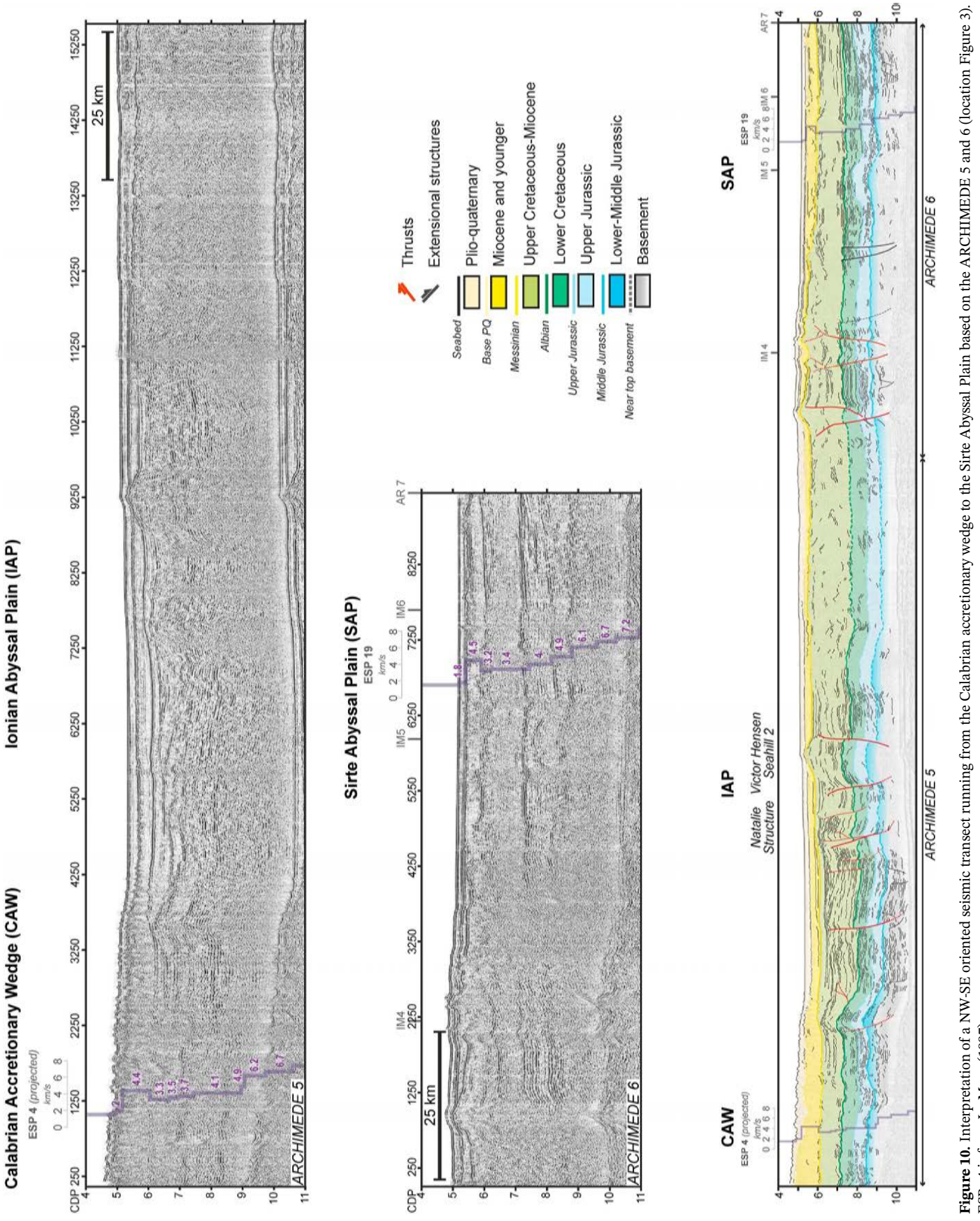

Figure 10. Interpretation of a NW-SE oriented seismic transect running from the Calabrian accretionary wedge to the Sirte Abyssal Plain based on the ARCHIMEDE 5 and 6 (location Figure 3). ESPs 4 is from Le Meur (1997).

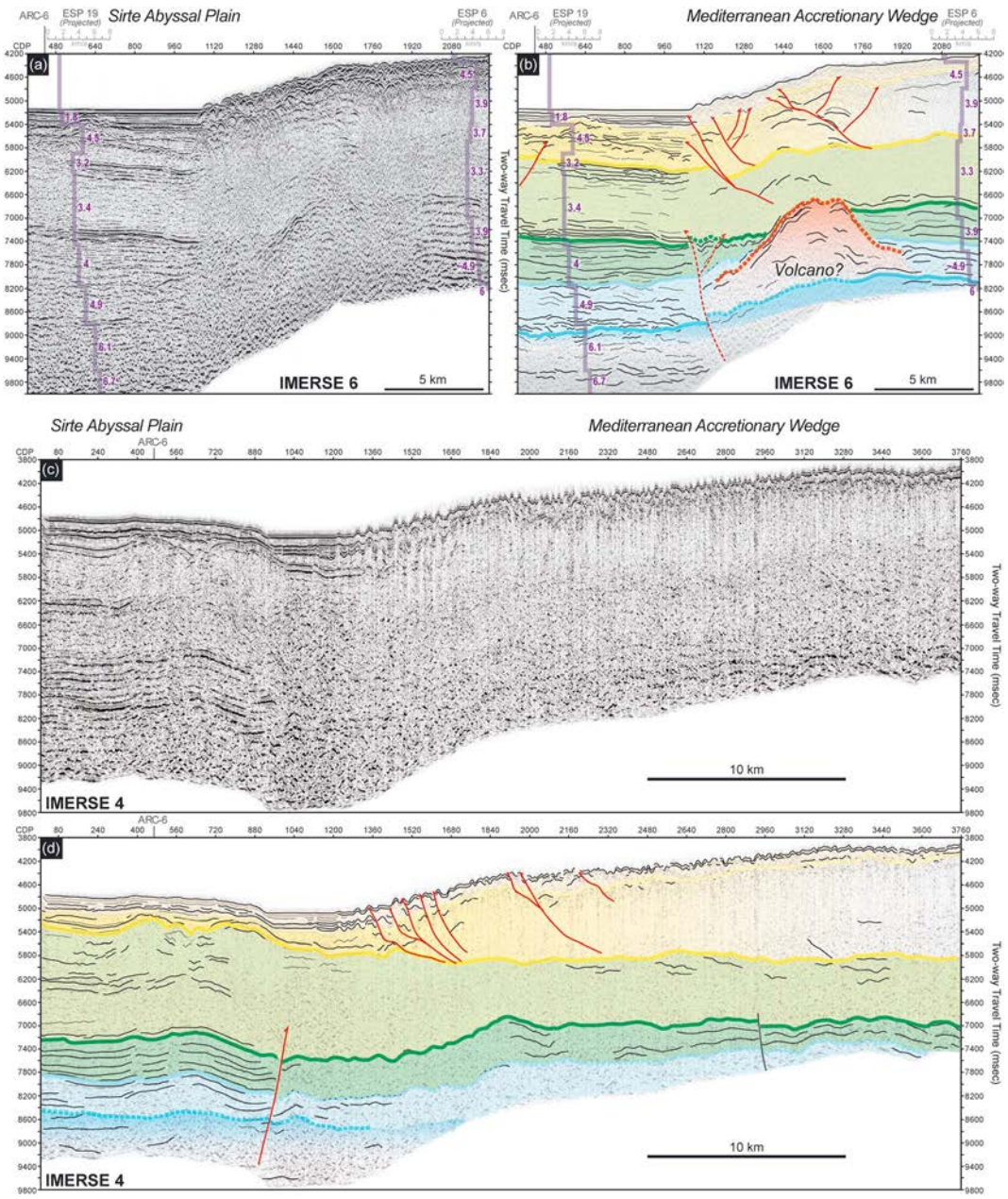

Figure 11. Interpretation of the IMERSE 4 and 6 seismic profiles (location in Figure 3). ESPs 19 and 6 are from Le Meur (1997). Same caption as Figure 10.

and beneath the Calabrian and Mediterranean wedges. Because most ESP models are projected on our seismic profiles, local misfits are observed, notably for the deepest sedimentary sequences (Figure 8).

5.1. Plio-Quaternary and Messinian Evaporitic Sequences

The Plio-Quaternary sequence corresponds to a package of subparallel, high-frequency, low-amplitude reflectors (Gallais et al., 2011; Hieke et al., 2003; Minelli & Faccenna, 2010) showing relatively homogeneous low seismic velocities (1.8–2.0 km/s; de Voogd et al., 1992 ; Le Meur, 1997). Its base is delimited by a high-amplitude reflector regionally identifiable and mappable (Figures 8–11) referred to as the M reflector (Polonia et al., 2002; Reston, Fruehn, et al., 2002; Reston, Von Huene, et al., 2002) or A reflector (Chaumillon et al., 1996; Finetti & Morelli, 1972) also corresponding to the E1-refracted phase of de Voogd et al. (1992). Drilled at DSDP Site 374, the Plio-Quaternary sequence mainly consists of terrigenous

and turbidite deposits (Figure 3a; Hsu et al., 1978). Its thickness ranges from 100 to 300 m within the Ionian and Sirte Abyssal plains (de Voogd et al., 1992; Le Meur, 1997). These sediments are nearly undeformed. In contrast, they appear faulted and folded close to the deformation front of the Mediterranean accretionary wedge (Figures 9 and 11; Reston, Fruehn, et al., 2002; Reston, Von Huene, et al., 2002) and within the internal part of the Calabrian wedge (Figure 10; Minelli & Faccenna, 2010). The Plio-Quaternary sediment thickness increases within the Calabrian and Hellenic fore-arc basins where they are affected by normal faulting and related salt activity (Figure 9; Minelli & Faccenna, 2010). The extensional and compressional features described above are caused by salt-related deformation and gravitational failure at the front and back of the wedges.

The Messinian evaporitic sequence includes a series of continuous weakly reflective reflectors on top of a transparent layer (Figure 8). The base is characterized by a continuous high-amplitude reflector of reverse polarity, referred as the B reflector or T reflector (Chaumillon et al., 1996; Finetti & Morelli, 1972; Polonia et al., 2002; Reston, Fruehn, et al., 2002; Reston, Von Huene, et al., 2002), also corresponding to the S1-horizon of de Voogd et al. (1992). In detail, based on this seismic facies change, two subunits are distinguished and referred to as the Upper and Lower Evaporites (Hsu et al., 1978) delimited by the E2-horizon in the velocity model of de Voogd et al. (1992). The Messinian evaporitic sequence is generally characterized by high velocities (~4.4–4.5 km/s, Figure 8), below which a velocity inversion is observed (Figure 8; Le Meur, 1997; de Voogd et al., 1992). Only the top of the Messinian evaporites was reached at DSDP Site 374 (Hsu et al., 1978). Considering the velocity models of Le Meur (1997), the Messinian evaporitic sequence thickness increases between the Sirte and Ionian abyssal plains (Figure 8) from 1.1 (ESP 19) to 1.9 km (ESP 5). This sequence clearly seals the deformation observed in the Ionian Abyssal Plain related to the formation of NE-SW oriented ridges (Figures 3 and 10; Nathalie structure, Victor Hensen Seahills 2; Chamot-Rooke, Rangin, et al., 2005; Gallais et al., 2011). We also found compressional deformation in the Sirte Abyssal Plain, where, in contrast to the Ionian Abyssal Plain, the Messinian evaporitic sequence seems to be folded (Figure 10). The base of this sequence represents an important decoupling horizon that partly controls the evolution of the Mediterranean (Figure 9; Chaumillon et al., 1996; Reston, Fruehn, et al., 2002; Reston, Von Huene, et al., 2002) and Calabrian accretionary wedges (Figures 6a/b and 10; Gallais et al., 2012; Minelli & Faccenna, 2010). Because of this decoupling interface, the sedimentary sequences of the Ionian Basin are relatively well preserved underneath and can be mapped quite far beneath both the Calabrian and Mediterranean wedges (Figures 8–11).

5.2. Upper Cretaceous to Miocene Sequence

The Upper Cretaceous to Miocene sequence shows seismic facies variations between the Sirte and Ionian abyssal plains (Figure 8). Characteristic velocities are quite similar (Figure 8; 3.2–3.4 km/s), despite slightly higher velocities (3.7 km/s) in the basal subunit of the Ionian Abyssal Plain. In the Sirte Abyssal Plain and beneath the Mediterranean Accretionary wedge, this sequence generally corresponds to a very weakly reflective package (Figure 8) locally interrupted by a succession of high-amplitude reflectors that are laterally continuous over tens of kilometers (Figures 7 and 11). The top of this sequence is characterized by a series of high-amplitude reflectors (Figures 8 and 11) with velocities of 3 to 3.2 km/s (ESP 19, Figure 8; de Voogd et al., 1992; Le Meur, 1997). Its base corresponds to remarkable high-amplitude reflectors (referred to as the K-reflector in Chaumillon et al., 1996; Polonia et al., 2002; Reston, Fruehn, et al., 2002; Reston, Von Huene, et al., 2002) also marked by a velocity increase from 3.3–3.4 to 3.9–4 km/s (Figure 8; Le Meur, 1997). The K-horizon is classically interpreted as the base of Tertiary sediments (Polonia et al., 2002; Reston, Fruehn, et al., 2002; Reston, Von Huene, et al., 2002); however, in our work, this horizon correlates well with the Albian age calibration derived from the Sirte Basin (Figure 7). In the Ionian Abyssal Plain (Figure 8) and beneath the Calabrian wedge, close to the Malta escarpment (Figure 6b; Minelli & Faccenna, 2010), the Upper Cretaceous to Miocene sequence is well layered and characterized by a succession of discontinuous high amplitude reflectors. The top of the sequence has velocities of 3 to 3.2 km/s (Le Meur, 1997; de Voogd et al., 1992), similar to what is observed in the Sirte Abyssal Plain (Figure 8). Its base is correlated to the Albian horizon calibrated from the Malta escarpment (Figure 6b). In our interpretation, the base of this sequence does not correspond to the K-reflector identified in the Ionian Abyssal Plain (see comparison in Gallais et al., 2011).

The upper subunit of Upper Cretaceous to Miocene sequence (v ~ 3–3.2 km/s, Figure 8) has recently been reinterpreted as corresponding to Lower Messinian units (Gallais et al., 2011), based on similarities to seismic facies described by Lofi et al. (2011). Below this subunit, syntectonic sequences recording pre-Messinian compression in the Ionian Abyssal Plain are well developed (Chamot-Rooke, Rangin, et al., 2005; Gallais et al., 2011; Pagot et al., 1999; Sioni, 1996), but they cannot be traced confidently towards the Sirte Abyssal Plain, where deformation is less severe (Figure 10).

At the scale of the Ionian Basin, the base of the Upper Cretaceous to Miocene sequence consistently lies at about 7 s (twtt; Figures 7–11), except in the Ionian Abyssal Plain (Figure 8), where it lies slightly deeper. The base of this sequence represents locally a remarkable decoupling interface, in particular near the Cyrenaica Ridge, where it acts as a decoupling layer for the listric faults identified within the sequence (Figure 7), but also within the inner part of the Mediterranean Accretionary Wedge (Figure 9). Here, the role of Albian sediments as a decoupling layer is corroborated by the recovery of Aptian (Ryan et al., 1982) up to Cenomanian pelagic shales (Kioka et al., 2015) within breccia samples cored in mud volcanoes, located near the contact with the backstop of the Mediterranean accretionary wedge (Figure 3; Chamot-Rooke, Rangin, et al., 2005; Rabaute & Chamot-Rooke, 2007).

5.3. Lower Cretaceous and Upper Jurassic Sequence

The Lower Cretaceous sequence generally appears well layered, characterized by relatively continuous and moderately reflective subhorizontal reflectors (Figures 6b and 7–11). Its base is indicated by a velocity increase from 3.9–4 km/s to 4.7–4.9 km/s (Le Meur, 1997), coinciding quite clearly with a high-amplitude reflector (Figures 8–11) correlated with the Upper Jurassic horizon calibrated along the Malta escarpment (Figure 6b).

The underlying sequence is suggested to correspond to Upper Jurassic sediments (Figures 6 and 8). It is also well layered and shows laterally continuous, relatively reflective subhorizontal reflectors (Figure 8). Because of its relatively high velocity (4.7–4.9 km/s), this layer was interpreted as basalts from the oceanic crust (Layer 2a) based on early refraction models (de Voogd et al., 1992) but a sedimentary origin as latter suggested (Le Meur, 1997). The base of this sequence is marked by discontinuous high-amplitude reflectors correlated with a velocity jump from 4.7–4.9 to 6.1 km (Figure 8) previously interpreted as the top of oceanic crust (Polonia et al., 2002; Reston, Fruehn, et al., 2002; Reston, Von Huene, et al., 2002).

Regional seismic transects across the Ionian Basin (Figures 9 and 10) suggest a relatively constant thickness for these two sequences (Figure 8). Because no drill hole reached these deep sedimentary sequences, indirect insights on lithologies may either come from the adjacent margins (Figure 5) or from clasts recovered from mud volcano eruptions (Chamot-Rooke, Rangin, et al., 2005; Kioka et al., 2015; Ryan et al., 1982). Nannofossils in cored clasts are as old as Late Jurassic to Early Cretaceous (Kioka et al., 2015). Dominant lithologies include shale, siltstone, and minor limestone (Kioka et al., 2015), similar to lithologies drilled in basinal parts of the Cyrenaica margin (Figures 4 and 5).

5.4. Lower to Mid Jurassic Sequence and Basement

Our cross-correlation work suggests the occurrence of an older and deeper sedimentary sequence underneath the Upper Jurassic sequence (Figures 6–11). The top of the oldest sequence can be correlated to the Middle Jurassic Horizon calibrated along the Malta escarpment (Figure 6b). This sequence, not always well imaged, is characterized by a series of discontinuous low-frequency reflectors found as deep as 9 s (twtt) in the Sirte Abyssal Plain (northeastern end of line ARCHIMEDE 7, Figure 7; southeastern end of line ARCHIMEDE 6, Figure 10). The base of this sequence is poorly defined but lies close to the 4.9- to 6.1-km/s velocity jump in the Sirte Abyssal Plain (ESP 19, Figure 8; Le Meur, 1997). Farther to the northwest, beneath the Calabrian wedge, the base of the sequence also seems to be close to the same jump from 4.9 to 6.2 km/s (ESP 4, Figure 8). If not crystalline basement, these high velocities would suggest well-compacted sediments most probably of carbonate nature, since high velocities (~6 km/s) are not uncommon for well-cemented deep water carbonates with porosity under a few percent (e.g., Anselmetti & Eberli, 1993; Hairabian et al., 2014). Deep water carbonates and marls represent the age equivalent basinal facies deposited in the surrounding margins (Figure 5). The 6.1 km/s may fully be a crustal unit, but there is a (small) misfit between the top of this 6.1-km/s layer and the top basement inferred from reflection seismic data.

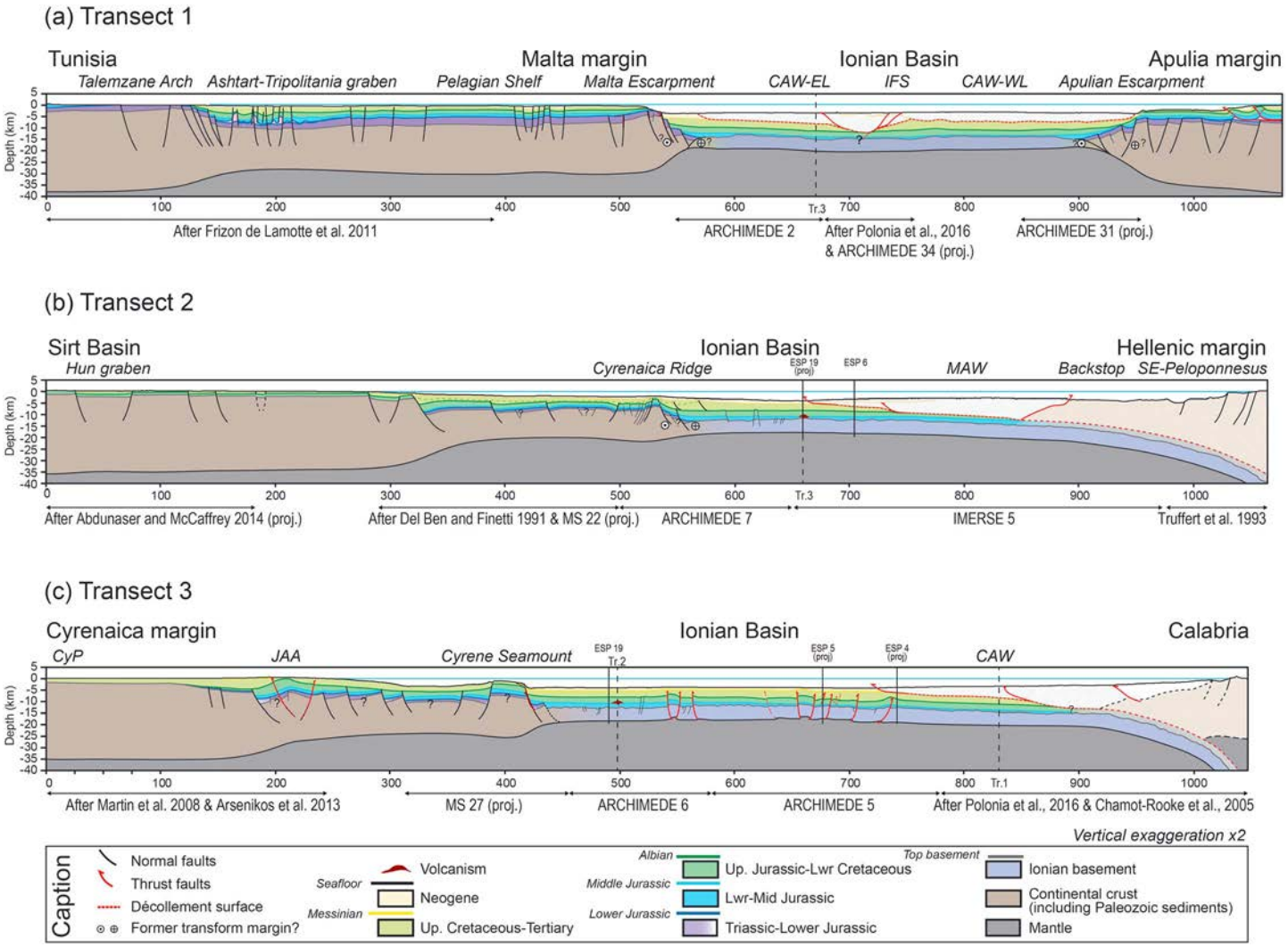

Figure 12. Regional transects across Ionian Basin and its margins (location in Figure 3). CAW: Calabrian Accretionary Wedge; MAW: Mediterranean Accretionary Wedge; CyP: Cyrenaica Platform; JAA: Jabal Al Akhdar. (a) Transect 1: Jeffara Basin, Malta and Apulia margins, and Ionian Basin. (b) Transect 2: Sirte and Ionian basins and Hellenic trench. (c) Transect 3: Cyrenaica margin, Ionian Basin, and Calabrian arc. CAW-EL: Calabrian Wedge-Eastern Lobe; CAW-WL: Calabrian Wedge-Western Lobe, IFS: Ionian Fault system (after Polonia et al., 2016).

This mismatch between the two types of seismic data may relate to seismic anisotropy, due to differences in vertical (reflection), and/or horizontal (refraction) velocities (Brittan & Warner 1996).

Despite uncertainties, our interpretation of the top basement is deeper than in previous studies (Gallais et al., 2011; Polonia et al., 2002; Reston, Fruehn, et al., 2002; Reston, Von Huene, et al., 2002). It is, however, similar to recent interpretations proposed by Polonia et al. (2011, 2017) in the Ionian Abyssal Plain based on deep reflection seismic data. In contrast to the interpretation of the top basement, the Moho depth is locally well constrained, marked by a refracted horizon corresponding to a velocity jump from 7.2 to 8.3–8.5 km/s on ESP data (Figure 8; Le Meur, 1997). Since our interpretation of the top basement is deeper than in previous studies, the overall crustal thickness is reduced and thinner than the 9–11 km of de Voogd et al. (1992; the 4.9 km/s is now interpreted as sediments rather than Layer 2A). It is also thinner than in Le Meur (1997; 7.4–7.7 km), since part of the 6.1 km/s may also be high-velocity sediments.

6. Deep Structure of the Ionian Basin and of Its Margins: Regional Transects

Regional transect locations were selected to maximize the benefit from reflection and refraction seismic profiles and/or existing geological sections (Figure 12). The first transect is oriented roughly SW-NE (Figure 3);

it shows the structure of the Malta and Apulian margins relative to the Ionian Basin and the chronological relationships with the structure of basins onshore Tunisia and on the Pelagian platform. The second transect is also oriented SW-NE and illustrates the structural and temporal relationships between the Sirte and Ionian basins. The third transect is roughly perpendicular to the two others; it shows the structure of the Cyrenaica margin and the spatial evolution of deep sedimentary sequences of the Ionian Basin.

6.1. Jeffara Basin, Malta, and Apulia Margins and Ionian Basin (Transect 1)

6.1.1. Geological and Geophysical Constraints for Transect 1

Transect 1 runs from basins onshore Tunisia to the Apulian continental margin, documenting an area of the Ionian Basin where the relationship to its former passive margins (Malta and Apulia) is preserved. We build on the work of Frizon de Lamotte et al. (2011) and Raulin et al. (2011) to show the crustal and stratigraphic architecture from basins onshore Tunisia to the offshore Pelagian and Malta platforms. The transition from the Malta platform to the Ionian Basin across the Malta escarpment is based on our calibration work (Figure 6a) and previous observations (Cernobori et al., 1996; Chamot-Rooke, Rangin, et al., (2005); Minelli & Faccenna, 2010; Polonia et al., 2011. The crustal structure of the Malta escarpment is mainly constrained by the refraction seismic profile shown by Dellong et al. (2018). The interpretation across the Ionian Basin is based on lines 2 and 34 from the ARCHIMEDE survey presented in Chamot-Rooke, Rangin, et al. (2005) and Gallais et al. (2013). The shallow structure of the Calabrian Prism is based on Polonia et al. (2016). The Moho depth is approximated from Chamot-Rooke, Rangin, et al. (2005). The transition from the Ionian Basin to the Apulian platform across the Apulian escarpment follows our interpretation of ARCHIMEDE 31 (Figure 6a) and complementary observations from Argnani (2013), Del Ben et al. (2015), Chamot-Rooke, Rangin, et al. (2005), and Minelli and Faccenna (2010).

6.1.2. Key Observations and Interpretations

We consider the basins onshore the Tunisian and Pelagian shelf to be part of the southern margin of the Ionian Basin (Figure 12a). Constraints on crustal thickness are solely derived from indirect methods (e.g., gravity inversion; Cowie & Kusznir, 2012). The thick sediment deposition evidenced offshore Tunisia indirectly suggests a significant crustal thinning (Figure 12a; Frizon de Lamotte et al., 2011; Raulin et al., 2011). A thick sedimentary cover is also observed over the Pelagian shelf (Jongsma et al., 1985) even if crustal thinning seems less important toward the Malta escarpment (Figure 12a; see global map in Cowie & Kusznir, 2012). Field observations in Tunisia (Talemzane Arch and Jeffara plain) combined with seismic interpretations in the Ashtart-Tripolitania graben suggest that the main rift event occurred during the Late Triassic to Early Jurassic (Frizon de Lamotte et al., 2011; Raulin et al., 2011; Figure 12a). A renewed episode of rifting occurred offshore Tunisia and over the Pelagian shelf during the Early Cretaceous (Jongsma et al., 1985). Neogene transtensional motions resulted in the formation of the Malta, Linosa, and Pantellaria rift basins over the Pelagian platform (Figures 3 and 12a; Casero & Roure, 1994; Chamot-Rooke, Rangin, et al., 2005; Jongsma et al., 1985).

The Malta and Apulian margins both show an abrupt morphological transition to the Ionian Basin. This led Frizon de Lamotte et al. (2011) to interpret the Malta escarpment as a transform boundary accompanying the opening of the Ionian Basin and more generally consistent with NW-SE trending segments of the southernmost Tethyan margin. Based on recent refraction data (Dellong et al., 2018), the sharp morphology of the Malta escarpment coincides at depth with a sharp crustal neck occurring within ~20-km distance (Figure 12a). No refraction data are available on the Apulian side, but the abrupt linear trend of the margin, despite reshaping during the Messinian erosion, is preserved. Refraction data of Dellong et al. (2018) also image a sharp ocean-continent transition and the tabular architecture of the Ionian crust. Our section runs south of the Alfeo-Etna fault system (Figures 1 and 3; Polonia et al., 2016) commonly interpreted as a STEP fault (Cernobori et al., 1996; Hirn et al., 1997; Argnani et al., 2002; see review in Gallais et al., 2013) and consequently does not show it. Polonia et al. (2016) suggested an alternative location for the STEP fault farther east, at the location of the Ionian fault system (Figures 1 and 3). Evidence of rifting is recorded in the Late Triassic-Early Jurassic units over the Malta and Apulian margins (Figures 5 and 6), while the first sedimentary sequence mapped over the Ionian Basin is latest Early Jurassic to Middle Jurassic in age (Figures 6 and 8).

6.2. Sirte and Ionian Basins (Transect 2)

6.2.1. Geological and Geophysical Constraints for Transect 2

Transect 2 extends from the onshore Sirte Basin to the Hellenic subduction system. Onshore, the architecture of the Sirte Basin is based on studies by Abadi et al. (2008) and Abdunaser and McCaffrey (2014).

The offshore crustal and stratigraphic architecture is less constrained. Here we rely on the MS22 seismic profile (Finetti & Morelli, 1972), also using the work of Del Ben and Finetti (1991). The transition from the Sirte to the Ionian Basin across the Cyrenaica Ridge is further constrained by observations from the ARCHIMEDE 7 seismic profile (Figure 7). The structure of the Ionian Basin sequences and their integration in the Mediterranean accretionary wedge is based our interpreted IMERSE 5 seismic profile (Figure 9). The transition toward the Hellenic subduction system is based on the work of Truffert et al. (1993). The Moho depth is well constrained in the vicinity of the ESP 19 and 6 by a refracted phase at ~18- to ~19-km depth (Le Meur, 1997; de Voogd et al., 1992).

6.2.2. Key Observations and Interpretations

We consider the Sirte Basin to be part of southern margin of the Ionian Basin, east of the Medina escarpment (Figure 12a). A significant change in crustal structure is observed from the onshore to the offshore Sirte Basin (Figure 12b): Thinning was limited onshore, whereas the crust is locally less than 15 to 20 km thick offshore (Figure 12b; Cowie & Kusznir, 2012). The main structures of the offshore Sirte Basin are clearly visible in the free-air gravity field (Figure 3b). Despite limited constraints on the timing of the offshore Sirte Basin rifting, it is commonly accepted that the main rift event and associated subsidence occurred during the latest Jurassic to Cretaceous (Abadi et al., 2008; Abdunaser & McCaffrey, 2014; Anketell, 1996; Wennekers et al., 1996), explaining the thick sedimentary sequences evidenced along the transect (Figure 12b). An earlier Triassic rift event is documented (Del Ben & Finetti, 1991; Massa & Delort, 1984; Thusu, 1996; Wennekers et al., 1996), but this early event likely led to insignificant subsidence.

The Cyrenaica Ridge delimiting the Sirte and Ionian basins is mapped as a narrow structural high also showing as a positive anomaly in the free-air gravity map (Figures 3b, 7, and 12b). The transition toward the deep flat stratified sequences of the Ionian Basin in the Sirte Abyssal Plain is quite abrupt, occurring within a few tens of kilometers (Figure 12b). This suggests a shear origin for the ridge itself, either as transtension or pure transform. Immediately northeast of the Cyrenaica ridge, a set of large listric faults affects the upper sedimentary cover (Upper Cretaceous to Tertiary). We infer that they root along the Albian horizon acting as a décollement layer (Figures 7 and 12b). Since these faults are sealed by the base Tertiary (Figure 7), they are likely Upper Cretaceous in age and possibly contemporaneous with the main rifting episode recorded in the Sirte Basin. In addition to these listric faults, pre-Tertiary steep normal faults affect the entire pre-Albian sequences.

Diachronous formation of the Ionian and Sirte basins is a key element of Transect 2 (Figure 12b). Rifting in the Sirte Basin is early Late Cretaceous, while the first sequences flooring the Ionian basin are Early Jurassic to Middle Jurassic. Farther to the northeast, upper sequences of the Ionian Basin are incorporated into the Mediterranean accretionary wedge as the décollement level steps down from the Messinian unit at the toe of the prism to deeper sequences (Figures 9 and 12; Truffert et al., 1993). The main décollement may locate within the Albian shales (Ryan et al., 1982; Truffert et al., 1993) favoring the formation of duplexes within the wedge (Reston, Fruehn et al., 2002).

6.3. Cyrenaica Margin and Ionian Basin (Transect 3)

6.3.1. Geological and Geophysical Constraints for Transect 3

Transect 3 extends from the Cyrenaica platform to the Calabria subduction. Much of this transect follows the work of Frizon de Lamotte et al. (2011), although it is differently oriented to clarify the transition from the Cyrenaica margin to the deep Ionian Basin. The shallow structure of the Cyrenaica platform and the Jabal Al Akdar anticline relies on Arsenikos et al. (2013) and Martin et al. (2008). Stratigraphy is less well-constrained offshore Cyrenaica and toward the Cyrene Seamount, and deeper structures at crustal level remain essentially unknown. Projected MS 27 profile (Finetti & Morelli, 1972) and ARCHIMEDE Profiles 5 and 6 (Figure 10) are used across the Ionian Basin. First-order structure toward Calabria follows the interpretation of Chamot-Rooke, Rangin, et al. (2005) and Polonia et al. (2016).

6.3.2. Key Observations and Interpretations

The sedimentary record of the Cyrenaica margin rifting has to be looked for offshore. However, the margin was inverted during the Late Cretaceous and Middle to Late Eocene (Arsenikos, 2014; Arsenikos et al., 2013) so that part of it is now exposed onshore (Figure 12c; e.g., Jabal Al Alkdar antiform). Significant thickening of pre-Upper Cretaceous sedimentary has been found in wells (Arsenikos et al., 2013; Martin et al., 2008; Yanilmaz et al., 2008) suggesting that some crustal thinning occurred onshore, although moderate

(Figure 12c). Most of the crustal thinning occurred offshore and toward the Cyrene Seamount, interpreted as a marginal high (Groupe-Escarmed et al., 1987). Two main rift events are described over the Cyrenaica margin. The older one is Triassic to Early Jurassic (Arsenikos, 2014; Keeley & Massoud, 1998; Yanilmaz et al., 2008) contemporaneous with the formation of both the Talemzane Arch onshore Tunisia (Raulin et al., 2011) and the Malta/Apulian margins (Figure 6 and 12). The second rifting occurred in the Early Cretaceous (Arsenikos et al., 2013) in the range of age accepted for the Sirte Basin (Abadi et al., 2008; Abdunaser & McCaffrey, 2014; Anketell, 1996; Wennekers et al., 1996). Limited constraints are available to unravel the transition from the Cyrene Seamount to the deeper Ionian Basin, but part of the structuration of the Cyrene Seamount seems to have occurred in the early Late Cretaceous as recorded by a correlative deepening of the depositional environments (Figure 4; Biju-Duval et al., 1982; Charier et al., 1987; Groupe-Escarmed et al., 1987). The oldest sequences that can be mapped across the entire transect are late Early Jurassic to Middle Jurassic (Figures 10 and 12c), although sequences as old as Triassic to Early Jurassic might be preserved close to marginal highs such as the toe of the Cyrene Seamount.

This transect crosses the Miocene compressive structures previously mapped near the Medina Seamount and south of the Cephalonia fault (Figure 3) in the Ionian Abyssal Plain (Chamot-Rooke, Rangin, et al., 2005; Gallais et al., 2011; Pagot et al., 1999). We show here that the same deformation is observed farther south within the Sirte Abyssal Plain, although less severe (ARCHIMEDE 6, Figure 10). Reverse faults, roughly oriented NE-SW, have been interpreted as inverted oceanic normal faults (Gallais et al., 2011). Inversion, clearly recorded by pre-Messinian wedged syntectonic sequences, could be Tortonian (Chamot-Rooke, Rangin, et al., 2005; Gallais et al., 2011), contemporaneous with the fast phase of opening of the Tyrrhenian Basin. Based on some compressive deformation observed offshore Tunisia, Roure et al. (2012) proposed an older late Oligocene age. However, this would require a condensed Miocene section, which sounds quite improbable taking into account that the Miocene is the time of construction of the nearby Mediterranean Ridge and progressive burying of the African plain. Farther to the southeast, toward the Sirte Abyssal Plain, sequences as young as Messinian are deformed, suggesting that compressional deformation continued during the early Messinian (Figures 10 and 12).

7. Discussion

7.1. Age of the Ionian Basin

The correlation of sedimentary sequences across the Ionian Basin combined with the age calibrations conducted at the adjacent margins constrains the age of the Ionian Basin to the late Early Jurassic to Middle Jurassic time. This age is compatible with the deepening of the paleobathymetries documented along the Malta escarpment (Biju-Duval et al., 1982; Charier et al., 1987) and within the Apulian platform (Figure 5). This major subsidence was accompanied with the widespread occurrence of Middle to Late Jurassic pillow lavas and basalts over the Malta shelf and escarpment (Biju-Duval et al., 1982; Charier et al., 1987). We relate this volcanism to the onset of oceanic spreading in the Ionian Basin. The Cyrenaica margin was already deep in Middle Jurassic time, but we could not calibrate the onset of subsidence.

The age suggested in this work is compatible with the geophysical data available in the Ionian Basin and expected to depend on the age of lithosphere, that is, surface heat flow and depth to the basement. The mean heat flow of the Ionian Basin is 36 or 44 mW/m^2 once crudely corrected from sedimentation effects (details of the calculations can be found in Chamot-Rooke, Rangin, et al., 2005). This is colder than the mean 50 $\pm$ 10-mW/m^2 heat flow reported for old (120 to 160 Ma) oceanic lithosphere; Parsons & Sclater, 1977; Stein & Stein, 1992). The calculated unloaded Ionian basement depth would be between 6,700 and 7,000 m, a value deeper than the mean ocean floor depth reported for the oldest oceanic lithosphere (5,600 $\pm$ 500 m; Stein & Stein, 1992). Surface heat flow values and depth to the basement are thus not incompatible with a Lower Jurassic to Middle Jurassic oceanic lithosphere flooring most of the Ionian Basin, providing cooling and subsidence follow a square root of age relation with time (half-space cooling model rather than plate model) in an overall cold mantle environment (African Panafrican basement).

The late Early Jurassic to Middle Jurassic age suggested in this work is younger than the preferred age derived from magnetic modeling by Speranza et al. (2012), but not incompatible. Speranza et al. (2012) pointed out that any reverse polarity models in the range 290–190 Ma could reproduce the main magnetic

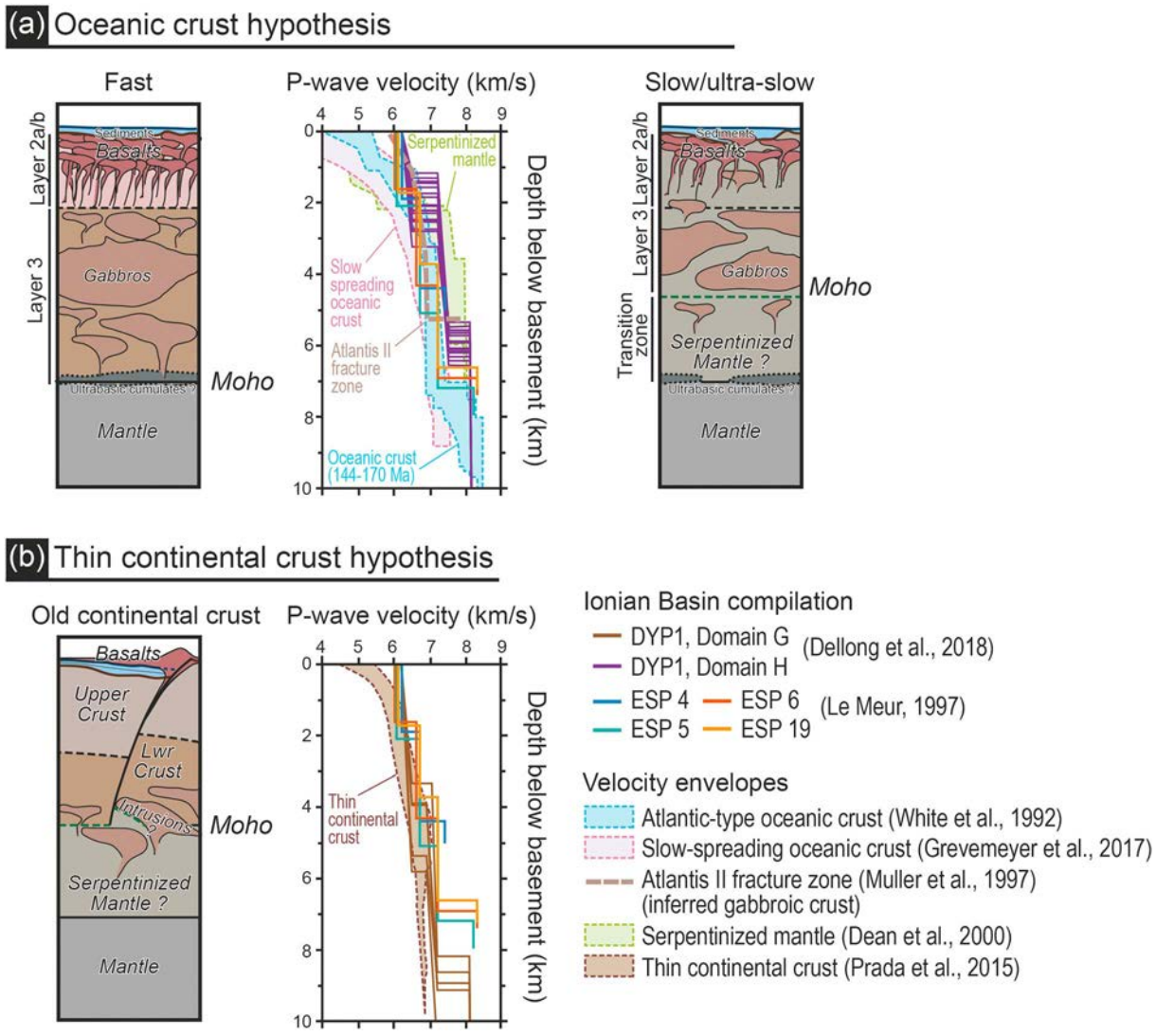

Figure 13. Comparison between the (a) oceanic (fast versus slow/ultraslow) versus (b) thin continental crust hypothesis based on information on the velocity structure of the Ionian Basin. Each hypothesis is associated with simplified logs showing interpreted lithologies that could explain the observed velocity structure. One-dimensional velocity models are based on ESPs results (Le Meur, 1997) and extracted from the DYP1 refraction profile (Dellong et al., 2018). Blue-shaded area represents the velocity envelope from mature Atlantic-type oceanic crust (144–170 Ma, White et al., 1992). Pink-shaped area corresponds to the velocity envelope of oceanic crust found at slow-spreading ridges as compiled by Grevemeyer et al. (2018). Green-shaded area corresponds to the velocity envelope of serpentinized mantle presented by Dean et al. (2000). Brown-shaded area represents the velocity envelope compiled by Prada et al. (2015) for thin continental crust. Dashed light-brown curve represents the 1-D depth-velocity profile determined by Muller et al. (1997) near the Atlantic II fracture zone close to drilled gabbroic bodies.

feature observed in the Ionian Basin. They selected the predominantly reverse polarity interval of Carnian time (E8r-E12r, 227 to 219 Ma, Figure 2), but the younger Norian/Rhaetian period of dominantly reverse intervals (E17r-E20r, 205 to 210 Ma, Figure 2) could equally fit (chrons are from Kent & Olsen, 1999). Latest Triassic and earliest Jurassic times comprise predominantly normal polarity intervals (Kent & Olsen, 2008), but one long-enough reverse interval is present in all of the early Jurassic stages (Sinemurian, Pliensbachian, and Toarcian, from 195 to 175 Ma, Figure 2). In contrast, these ages are definitely different from the 340-Ma age proposed by Granot (2016) for the Herodotus Basin, based on the limited information contained in the skewness of one single prominent magnetic anomaly. We cannot totally rule out that the three main basins (Ionian, Herodotus, and Levant) were formed at different ages (as suggested for the Levant and Herodotus basins in Segev et al., 2018), but stratigraphic similarities along the entire southern margin argue for a common origin. The eastern Mediterranean is clearly lacking a good knowledge of the magnetic field at short wavelength to resolve relationships between basins.

7.2. Nature of the Ionian Crust

The nature of the Ionian Basin crust is a long-lasting debate. Despite the absence of undisputedly recognized magnetic lineations, most authors seem to prefer the oceanic interpretation. Until recently, crustal thickness remained the only argument, rather than the velocity structure of the crust itself. Potential methods (gravity inversion and magnetics) reached two important conclusions for the Ionian Basin: (1) The crust is thin (<10 km), regardless of its nature (Cowie & Kusznir, 2012), and (2) magnetic modeling requires an oceanic-type magnetization (Speranza et al., 2012). Direct evidence for thin crust (i.e., seismic) has been obtained for the Ionian and Sirte abyssal plains (Dannowski et al., 2019; de Voogd et al., 1992; Lallemant et al., 1994; Le Meur, 1997; Truffert et al., 1993), as well as offshore Sicily and across the Malta escarpment (Dellong et al., 2018; Makris et al., 1986; Nicolich et al., 2000).

We tested the velocity structures of the ESPs for both continental and oceanic origin (Figure 13) using the models of Le Meur (1997) and our interpreted top basement (i.e., top of the 6.2 km/s for ESP 4 and considering 750 m of sediments as part of the 6 km/s for the ESPs 5, 6, and 19). Following many others, and based on our age calibration, we conclude that the thin Ionian crust shows similarities with old oceanic crust (Lower to Middle Jurassic), at least where ESP data are located. Results from recent wide-angle seismic experiments (Dannowski et al., 2019; Dellong et al., 2018) confirm the oceanic nature of the Ionian crust, discarding the continental crust hypothesis east of the Malta escarpment and north of the Medina Seamount where they interpret the location of the ocean-continent transition.

However, the results also suggest that the Ionian Basin basement may not be *standard* oceanic crust, since high velocities prevail in the upper part of the crust where oceanic layers 2A/B are expected (Figure 13). The observed crustal velocities are on the higher side of global compilations (Grevemeyer et al., 2018; White et al., 1992), perhaps because these compilations do not include oceanic crusts as old as the one considered here. The evolution of the petrophysical properties of the oceanic crust with time is poorly constrained. Porosity in basalts is expected to decrease with age due to porosity closure (Carlson & Herrick, 1990), an effect likely to affect the velocity gradient generally observed in oceanic Layer 2. Velocities higher than 5 km/s and up to 6 km/s in the uppermost oceanic crust have been measured in several basins, such as the Algerian Basin (Aïdi et al., 2018), the Tagus Abyssal Plain (Afilhado et al., 2008), or the volcanic slow-spreading segments of the Labrador Sea (Delescluse et al., 2015). These atypical velocities were interpreted as evidence for slow-spreading environments, and in the case of the Labrador Sea, slow- to ultraslow-spreading rates were actually proven (see synthesis in Delescluse et al., 2015). The oceanic crust formed at slow- to ultraslow-spreading centers tends to be a mix of partly serpentinized mantle and intrusive gabbroic plutons (Figure 13; Cannat, 1996). The exposure of gabbroic intrusions at the seafloor may explain local higher velocities in the upper oceanic crust (Figure 13) close to fracture zones (Muller et al., 1997). Serpentinite diapirs near fault contacts (Polonia et al., 2017), and atypical velocity structure (Dellong et al., 2018), led these authors to suggest that the Ionian oceanic crust formed at a slow-spreading ridge. The atypical Ionian crust may thus relate to both initial slow-spreading regime and postaccretion evolution with aging. Furthermore, the Ionian Basin likely formed subsequent to breakup in an overall cold environment (Panafrican Basement). The absence of constraint on spreading rate estimates prevents a direct confirmation of the slow-spreading hypothesis.

7.3. The Ionian Basin in the Context of the East Mediterranean Evolution

7.3.1. Kinematic Context

Paleomagnetic studies found no clear evidence for differential rotation between Adria and Africa since the Early Cretaceous time, with the exception of a modest post-Eocene counterclockwise rotation (Channell, 1996; Rosenbaum et al., 2004; Van Hinsbergen et al., 2014). Adria and Africa actually seem to share the same paleomagnetic poles since the Early Permian, although this conclusion is based on a limited number of samples for parautochthonous Adria (Muttoni et al., 2013). Paleolatitudinal shift between Adria and Africa is difficult to extract from paleomagnetism, which is inherent to the relatively small north-south extent of the Ionian Basin. Treating Adria as one single rigid block has proven to be challenging in the paleoreconstructions of the Alpine domain (Le Breton et al., 2017; Van Hinsbergen et al., 2014). If attached to Africa, Adria remains too far south (see discussion in Handy et al., 2010, and Le Breton et al., 2017). A number of scenarii thus include post-Eocene NE-SW extension between Adria and Africa, which would require intraplate deformation of the Ionian Basin lithosphere amounting to 60 to 420 km. The reverse fault system that reactivated the spreading fabric of the Ionian Basin near the Medina Seamounts (or Medina

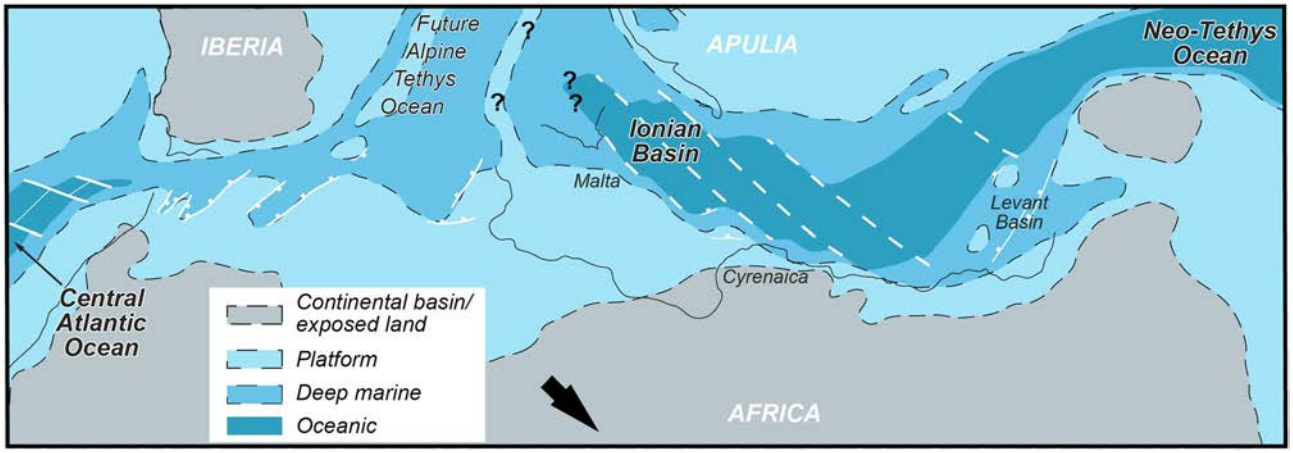

Figure 14. Tectonic context related to the formation of the Ionian Basin during Middle Jurassic time. The Ionian Basin formed during a late propagation of the Neo-Tethys Ocean, contemporaneous with the central Atlantic opening. The black arrow represents the movement of Africa relative to fixed Europe during Middle Jurassic time. Modified after Frizon de Lamotte et al. (2011), Guiraud et al. (2005), and Leprêtre et al. (2018).

Ridge) may have accommodated a component of strike slip, but no clear evidence for extension within the basement has been found so far. If at all present, Neogene intraplate deformation may be buried beneath the Calabrian or Mediterranean wedges or, alternatively, Adria may have been fragmented into several blocks, both hypothesis being evaluated in Le Breton et al. (2017).

Our age calibrations suggest that the Ionian Basin formed in the late Lower Jurassic to Middle Jurassic after a Triassic to Lower Jurassic rifting phase recorded over the adjacent margins (Figure 5). This timing overlaps with the age of the opening and propagation of the Central Atlantic oceanic basin, which separated North America/Europe from the African plate (Biari et al., 2017; Labails et al., 2010). A crucial constraint for the kinematics of opening of the Ionian Basin, and more generally for the opening of the eastern Mediterranean Basins, is thus the relative motion of Africa with respect to Eurasia. The post-Cretaceous motion is quite well constrained using the magnetic anomalies of the Central Atlantic, in contrast to the Jurassic stage. The Ionian Basin opened during an overall left-lateral motion of Africa relative to Europe in relation with the opening of the Central Atlantic (Figure 14). According to Rosenbaum et al. (2004), transcurrent left-lateral motion was active between 175 Ma and anomaly M0 (120 Ma), after which Africa started to converge toward Eurasia. We speculate that this motion actually started with the early rifting of the Central Atlantic, that is, around 200 Ma (Sinemurian, Labails et al., 2010). The rifting of the Central Atlantic, left-lateral motion of Africa with respect to Eurasia and opening of the Ionian Basin are thus contemporaneous events. The corollary to this timing is that the early direction of the eastern Mediterranean Basins opening had to be compatible with the sense of shear, that is, NW-SE directed (Chamot-Rooke et al., 2005; Barrier et al., 2008; Frizon de Lamotte et al., 2011). This opening direction is compatible with the observed narrowness of the Malta margin (Dellong et al., 2018) and to some extent of the Apulian margin, interpreted as formed in a transtensional to transform setting (Figure 12). The details of the segmentation and the associated partitioning of the deformation between transform, oblique, and orthogonal segments remain to be established in the Ionian Basin, but we can nevertheless conclude that the Malta and Apulian segments were initially not conjugate margins. The NW-SE direction of opening is now firmly established for the Levant and Egyptian margins at the same period (Gardosh et al., 2010; Garfunkel, 1998, 2004; Tassy et al., 2015). Le Pichon et al. (2019) recently proposed an end-member solution to this overall NW-SE opening of the eastern Mediterranean Basins. The eastern Mediterranean would have opened as a pull-apart between two major strike-slip faults, one running along the North African margin and the other following the Apulian escarpment and Hellenic margin. Rather than one single strike slip, our model suggests a set of oblique but not parallel transfer faults along the northern margin of Africa (Figure 14; Chamot-Rooke et al., 2005; Barrier et al., 2008; Frizon de Lamotte et al., 2011).

The coinciding opening of the Central Atlantic Ocean (Biari et al., 2017; Labails et al., 2010) and its propagation toward the Alpine Tethys where extension focused in the Middle Jurassic (Mohn et al., 2010, and

references therein) may have inhibited any farther westward propagation of the Ionian Basin and eastern Mediterranean Basins, in general, during the Late Jurassic (Figure 14). In that sense, the Ionian Basin, and possibly Herodotus Basin, represents narrow short-lived oceanic basins recording the formation of a transient plate boundary between Africa and Adria during the cessation of the Neo-Tethys propagation (Frizon de Lamotte et al., 2011). The junction between the Ionian Basin and Alpine Tethys at the end of spreading during the Late Jurassic is poorly documented and currently debated. The two systems could be connected through an oceanic passway (Frizon de Lamotte et al., 2011). However, the discovery of Tithonian to Late Cretaceous Gondwanian dinosaur tracks in the Apulian platform supports the presence of a narrow continental block connecting the African and Adriatic plate (Bosellini, 2002; Zarcone et al., 2010).

7.3.2. Impact of the Lower Cretaceous Extension

The Lower Cretaceous to early Upper Cretaceous rift event recorded over the Cyrenaica margin (Arsenikos et al., 2013), the Sirte Basin (Abadi et al., 2008), and basins onshore Tunisia (Gabtni et al., 2013; Figure 5) seems to have had a limited impact within the Ionian Basin itself (Figure 12). In the deep offshore, normal faults that recorded this event are restricted to the Sirte Abyssal Plain close to the transition with the Sirte Basin (Figures 7 and 10–12b). Most of these faults seem to root onto the Albian-Aptian shales, accommodating a limited amount of finite motion. The same type of structures is reported along the Egyptian margin close to the margin edge (Tari et al., 2012). Steckler and ten Brink (1986) addressed this type of selective reactivation close to former continental margins, with a specific application to the Levant margin. The strength of the lithosphere is minimum on the landward side of the hinge zone, whereas regions cored with mantle (i.e., where low-strength crust was replaced by high-strength mantle through stretching) remain rigid, including the oceanic lithosphere itself. Cretaceous rifting mainly involved parts of the margins that were previously weakly thinned during the Late Triassic-Early Jurassic rifting, while the Ionian Basin itself remained untouched, as predicted in Steckler and ten Brink model. An interesting implication is that the Ionian Basin lithosphere had already acquired sufficient strength at the time of the rejuvenation of the margin (Cretaceous), which would require more than ~60-My thermal equilibration (Leroy et al., 2008; Naliboff & Buiter, 2015). This is again fully compatible with the ages we propose. An additional structural explanation for the lack of significant Ionian Cretaceous deformation is that the original structures were inappropriately oriented relative to the N-S Cretaceous extension direction (Dercourt et al., 1993; Frizon de Lamotte et al., 2015; Jolivet et al., 2015), except in the vicinity of the approximately E-W trending Cyrenaica ridge (Figures 7 and 10–12b). Rheological and structural hypotheses are not mutually incompatible. At a regional scale, multiphase rifting with tectonic quiescence in between results in the individualization of continental ribbons along the margins (Naliboff & Buiter, 2015; Steckler & ten Brink, 1986). We infer that the Cyrenaica Ridge at large is one of these ribbons that more or less escaped the Cretaceous Sirte rifting.

8. Conclusions

Reexamination of wells, dredges, and dives data obtained at platforms and escarpments surrounding the Ionian Basin provides the basis for a comprehensive stratigraphic framework, which is extended to the deep offshore using both reflection and wide-angle seismic data. Calibration of the deepest reflectors and correlation of regional horizons allow us to build new regional geological transects across the entire basin, from the shallow African margin to the two wedges that now drape the Ionian Basin, that is, the Calabrian prism and the Mediterranean Ridge. Our main results are the following:

1. The Ionian Basin formed during the late Early Jurassic to Middle Jurassic following a Late Triassic to Early Jurassic rifting. Previous episodes of extension shaped the African margin but did not lead to significant thinning and subsidence. Summing up geophysical and geological arguments (crustal thickness, velocity structure, magnetics, heat flow, depth to the basement, distribution of tilted continental blocks, continuity of the deep basement reflectors, and style of reactivation), the deep basin is floored with oceanic crust of Jurassic age, possibly sharing similarities with slow-spreading ridges. Analogues of such an old oceanic lithosphere are scarce, and the postspreading petrophysical evolution toward old ages remains unknown.
2. The Ionian Basin rifting is contemporaneous with the Late Triassic-Jurassic rifting along the Levant margin, while the early seafloor spreading is contemporaneous with that of the Central Atlantic. The Ionian Basin, and most probably all three main eastern Mediterranean Basins (Ionian, Herodotus, and

Levant), opened as a transient secondary branch of the Neo-Tethys halted with the formation of the Alpine Tethys (Frizon de Lamotte et al., 2011). These openings accompanied the left-lateral motion of Africa with respect to Europe that started at the onset of Atlantic breakup, while shearing was accommodated as oblique transcurrent faults along the margin of Africa. The exact kinematics (rate, geometry, relationships between basins, and reconstructions) remain to be quantified.

3. The Ionian crust and margins recorded postspreading deformation probably related to changing force balance at northern subductions (Hellenic and proto-Hellenic and Calabrian) with successive periods of oceanic subduction (slab pulls) and continental collision or resistance to subduction. These include the Cretaceous opening of the Sirte Basin, subsequent inversion in the Late Cretaceous and late Eocene offshore Cyrenaic, and, finally, Miocene to recent inversion along the Medina Ridge. Sirte extension and inversions seem to have reactivated former structures in a selective way, depending on stress orientation and rheology. Inland Sirte opening isolated the marginal Cyrenaica Ridge, Cretaceous and Eocene compressions rejuvenated large-scale rift structures, while the most recent Miocene compression reactivated the oceanic spreading fabric within a narrow corridor offshore Calabria. In all cases, finite deformation remained small, pointing to a rigid deep Ionian Basin that escaped dislocation through time and remained a structuring backbone of the eastern Mediterranean.

Acknowledgments
This paper is a contribution of the Groupe Recherche Industrie (GRI) South Tethys margin, a research agreement between TOTAL on one hand and the Geological Laboratory of École normale supérieure in Paris (CNRS/PSL Research University); the Université Pierre et Marie Curie (UPMC), now Sorbonne Université; and the Université de Cergy-Pontoise (UCP) on the other. We thank G. Karner, C. Johnson, and M. Delescluse for stimulating discussions in an early stage of this work; A. Polonia, F. Klingelhoefer, and an anonymous referee for thoughtful reviews; and T. Schildgen for her detailed edition of the paper. GMT (Wessel et al., 2013) and QGIS (QGIS Development Team, 2015) free softwares were used in this work. Satellite gravity was extracted from Sandwell et al. (2014) files and global topographic grid from Becker et al. (2009); both are freely available from the website of the UCSD (https://topex.ucsd.edu/WWW_html/srtm30_plus.html). Logs from the Grifone 1, Puglia 1, and Aretusa 1 wells are available from the VIDEPI Project, 2016n.d. (http://unmig.sviluppoeconomico.gov.it/videpi/en/pozzi/pozzi.asp).

References

Abadi, A. M., van Wees, J. D., van Dijk, P. M., & Cloetingh, S. A. P. L. (2008). Tectonics and subsidence evolution of the Sirt Basin, Libya. *AAPG Bulletin*, *92*(8), 993–1027. https://doi.org/10.1306/03310806070

Abdunaser, K. M. (2015). Review of the petroleum geology of the western part of the Sirt Basin, Libya. *Journal of African Earth Sciences*, *111*, 76–91. https://doi.org/10.1016/j.jafrearsci.2015.07.005

Abdunaser, K. M., & McCaffrey, K. J. W. (2014). Rift architecture and evolution: The Sirt Basin, Libya—The influence of basement fabrics and oblique tectonics. *Journal of African Earth Sciences*, *100*, 203–226. https://doi.org/10.1016/j.jafrearsci.2014.06.020

Abdunaser, K. M., & McCaffrey, K. J. W. (2015). Tectonic history and structural development of the Zallah-Dur al Abd Sub-basin, western Sirt Basin, Libya. *Journal of Structural Geology*, *73*, 33–48. https://doi.org/10.1016/j.jsg.2015.02.006

Afilhado, A., Matias, L., Shiobara, H., Hirn, A., Mendes-Victor, L., & Shimamura, H. (2008). From unthinned continent to ocean: The deep structure of the West Iberia passive continental margin at 38°N. *Tectonophysics*, *458*(1–4), 9–50. https://doi.org/10.1016/j.tecto.2008.03.002

AGOCO (Arab Golf Oil Company) (1980). Geology of a stratigraphic giant—The Messlah oilfield. In M. J. Salem, & M. T. Busrewil (Eds.), *The Geology of Libya*, (Vol. II, pp. 521–536). London: Academic Press.

Aïdi, C., Beslier, M.-O., Yelles-Chaouche, A. K., Klingelhoefer, F., Bracene, R., Galve, A., et al. (2018). Deep structure of the continental margin and basin off Greater Kabylia, Algeria—New insights from wide-angle seismic data modeling and multichannel seismic interpretation. *Tectonophysics*, *728-729*, 1–22. https://doi.org/10.1016/j.tecto.2018.01.007

Anketell, J. M. (1996). Structural history of the Sirt Basin and its relationships to the Sabratah Basin and Cyrenaican platform, northern Libya. In M. J. Salem, A. S. El-Hawat, & A. M. Sbeta (Eds.), *First Symposium on the Sedimentary Basins of Libya, Geology of the Sirt Basin*, (Vol. 2, pp. 263–274). Amsterdam: Elsevier.

Anselmetti, F. S., & Eberli, G. P. (1993). Controls on sonic velocity in carbonates. *Pure and Applied Geophysics PAGEOPH*, *141*(2–4), 287–323. https://doi.org/10.1007/BF00998333

Argnani, A. (2013). The influence of Mesozoic Palaeogeography on the variations in structural style along the front of the Albanide thrust-and-fold belt. *Italian Journal of Geosciences*, *132*(2), 175–185. https://doi.org/10.3301/IJG.2012.02

Argnani, A., Bonazzi, C., & the MESC 2001 Crew (2002). Tectonics of Eastern Sicily offshore: Preliminary results from the MESC 2001 Marine Seismic Cruise. *Bollettino di Geofisica Teorica ed Applicata*, *43*, 177–193.

Arsenikos, S. (2014). Tectonic evolution and structure of the Cyrenaica margin, Libya (East Mediterannean), 300 pp., PhD thesis, Univ. de Cergy-Pontoise, Cergy-Pontoise, France.

Arsenikos, S., Frizon De Lamotte, D., Chamot-Rooke, N., Mohn, G., Bonneau, M. C., & Blanpied, C. (2013). Mechanism and timing of tectonic inversion in Cyrenaica (Libya): Integration in the geodynamics of the East Mediterranean. *Tectonophysics*, *608*, 319–329. https://doi.org/10.1016/j.tecto.2013.09.025

Barrier, E., Vrielynck, B., Bergerat, F., Brunet, M. F., Mosar, J., Poisson, A., & Sosson, M. (2008). Palaeotectonic maps of the Middle East: Tectono-sedimentary-palinspastic maps from Late Norian to Pliocene. Paris: Atlas of 14 maps at 1/18 500 000. CGMW, W..

Basilone, L., Frixa, A., Trincianti, E., & Valenti, V. (2016). Permian-Cenozoic deep-water carbonate rocks of the Southern Tethyan Domain. The case of Central Sicily. *Italian Journal of Geosciences*, *135*(2), 171–198. https://doi.org/10.3301/IJG.2015.07

Basilone, L., Morticelli, M. G., & Lena, G. (2010). Mesozoic tectonics and volcanism of Tethyan rifted continental margins in western Sicily. *Sedimentary Geology*, *226*(1–4), 54–70. https://doi.org/10.1016/j.sedgeo.2010.02.009

Basilone, L., Sulli, A., & Morticelli, G. (2016). Integrating facies and structural analyses with subsidence history in a Jurassic–Cretaceous intraplatform basin: Outcome for paleogeography of the Panormide Southern Tethyan margin (NW Sicily, Italy). *Sedimentary Geology*, *339*, 258–272. https://doi.org/10.1016/j.sedgeo.2016.03.017

Becker, J. J., Sandwell, D. T., Smith, W. H. F., Braud, J., Binder, B., Depner, J., et al. (2009). Global bathymetry and elevation data at 30 arc seconds resolution: SRTM30_PLUS. *Marine Geodesy*, *32*(4), 355–371. https://doi.org/10.1080/01490410903297766

Ben-Avraham, Z., & Ginzburg, A. (1990). Displaced terranes and crustal evolution of the Levant and the eastern Mediterranean. *Tectonics*, *9*(4), 613–622. https://doi.org/10.1029/TC009i004p00613

Ben-Avraham, Z., Ginzburg, A., Makris, J., & Eppelbaum, L. (2002). Crustal structure of the Levant Basin, eastern Mediterranean. *Tectonophysics*, *346*(1–2), 23–43. https://doi.org/doi:10.1016/S0040-1951(01)00226-8

Ben-Avraham, Z., Woodside, J., Lodolo, E., Gardosh, M., Grasso, M., Camerlenghi, A., & Vai, G. B. (2006). Eastern Mediterranean basin systems. *Geological Society, London, Memoirs*, *32*(1), 263–276. https://doi.org/10.1144/GSL.MEM.2006.032.01.15

Berkhout, A. J., & Verschuur, D. J. (1997). Estimation of multiple scattering by iterative inversion. Part I: Theoretical considerations. *Geophysics*, *62*(5), 1586–1595. https://doi.org/10.1190/1.1444261

Biari, Y., Klingelhoefer, F., Sahabi, M., Funck, T., Benabdellouahed, M., Schnabel, M., et al. (2017). Opening of the Central Atlantic Ocean: Implications for geometric rifting and asymmetric initial seafloor spreading after continental breakup. *Tectonics*, *36*, 1129–1150. https://doi.org/10.1002/2017TC004596

Biju-Duval, B., Letouzey, J., & Montadert, L. (1978). Structure and evolution of the Mediterranean Basins. In *Initial Reports of the Deep Sea Drilling Project*, (Vol. 42), 951–984. Washington, D.C.: U.S. Government Printing Office. https://doi.org/10.2973/dsdp.proc.42-1.150.1978

Biju-Duval, B., Morel, Y., Baudrimont, A., Bizon, G., & Bizon, J. J. (1982). Données nouvelles sur les marges du Bassin Ionien profond (Méditerranée Orientale). Résultats des campagnes Escarmed. *Revue de l'Institut Français du Pétrole*, *37*(6), 713–732. https://doi.org/10.2516/ogst:1982036

Bizon, G., Muller, C., & Vieban, F. (1985). Les sédiments mésozoïques et cénozoïques de mer Ionienne (campagne Escarmed 3: Escarpement de Malte, mont Alfeo et monts de Médine). Etude biostratigraphique: foraminifères, nannoplancton, microfaciès. *Revue de l'Institut Français du Pétrole*, *40*(4), 431–455. https://doi.org/10.2516/ogst:1985027

Bonnefous, J. (1972). Geology of the quartzitic "Gargaf Formation" in the Sirte Basin, Libya. *Bulletin du Centre de Recherches de Pau - SNPA*, *6*(2), 225–261.

Bortoluzzi, G., Polonia, A., Torelli, L., Arton, A., Carlini, M., Carone, S., et al. (2017). Styles and rates of deformation in the frontal accretionary wedge of the Calabrian Arc (Ionian Sea): Controls exerted by the structure of the lower African plate. *Italian Journal of Geosciences*, *136*(3), 347–364. https://doi.org/10.3301/IJG.2016.11

Bosellini, A. (2002). Dinosaurs "re-write" the geodynamics of the eastern Mediterranean and the paleogeography of the Apulia Platform. *Earth-Science Reviews*, *59*(1–4), 211–234. https://doi.org/10.1016/S0012-8252(02)00075-2

Bosworth, W., El-Hawat, A. S., Helgeson, D. E., & Burke, K. (2008). Cyrenaican "shock absorber" and associated inversion strain shadow in the collision zone of northeast Africa. *Geology*, *36*(9), 695–698. https://doi.org/10.1130/G24909A.1

Brittan, J., & Warner, M. (1996). Seismic velocity, heterogeneity, and the composition of the lower crust. *Tectonophysics*, *264*(1–4), 249–259. https://doi.org/10.1016/S0040-1951(96)00130-8

Camera, L., Ribodetti, A., & Mascle, J. (2010). Deep structures and seismic stratigraphy of the Egyptian continental margin from multi-channel seismic data. *Geological Society, London, Special Publications*, *341*(1), 85–97. https://doi.org/10.1144/SP341.5

Cannat, M. (1996). How thick is the magmatic crust at slow spreading oceanic ridges? *Journal of Geophysical Research*, *101*(B2), 2847–2857. https://doi.org/10.1029/95JB03116

Capitanio, F. A., Faccenna, C., Funiciello, R., & Salvini, F. (2011). Recent tectonics of Tripolitania, Libya: An intraplate record of Mediterranean subduction. *Geological Society, London, Special Publications*, *357*(1), 319–328. https://doi.org/10.1144/SP357.17

Carlson, R. L., & Herrick, C. N. (1990). Densities and porosities in the oceanic crust and their variations with depth and age. *Journal of Geophysical Research*, *95*(B6), 9153–9170. https://doi.org/10.1029/JB095iB06p09153

Casero, P., & Roure, F. (1994). Neogene deformations at the Sicilian–North African plate boundary. In F. Roure (Ed.), *Peri-Tethyan Platforms*, (pp. 27–50). Paris: Editions Technip.

Catalano, R., Di Stefano, P., & Kozur, H. (1991). Permian circumpacific deep-water faunas from the western Tethys (Sicily, Italy)—New evidences for the position of the Permian Tethys. *Palaeogeography, Palaeoclimatology, Palaeoecology*, *87*(1–4), 75–108. https://doi.org/10.1016/0031-0182(91)90131-A

Catalano, R., Doglioni, C., & Merlini, S. (2001). On the Mesozoic Ionian Basin. *Geophysical Journal International*, *144*, 49–64. https://doi.org/10.1046/j.0956-540X.2000.01287.x

Cernobori, L., Nicolich, R., Petronio, L., & Romanelli, M. (1996). Crustal image of the Ionian basin and its Calabrian margins. *Tectonophysics*, *264*, 175–189. https://doi.org/10.1016/S0040-1951(96)00125-4

Chamot-Rooke, N., Gaulier, J.-M., & Jestin, F. (1999). Constraints on Moho depth and crustal thickness in the Liguro-Provençal basin from a 3D gravity inversion: Geodynamic implications. *Geological Society, London, Special Publications*, *156*(1), 37–61. https://doi.org/10.1144/GSL.SP.1999.156.01.04

Chamot-Rooke, N., Rabaute, A., & Kreemer, C. (2005). Western Mediterranean Ridge mud belt correlates with active shear strain at the prism-backstop geological contact. *Geology*, *33*(11), 861. https://doi.org/10.1130/G21469.1

Chamot-Rooke, N., Rangin, C., Le Pichon, X., Rabaute, A., & DOTMED Working Group (2005). DOTMED—Deep offshore tectonics of the eastern Mediterranean: A synthesis of deep marine data in the eastern Mediterranean—The Ionian Basin and margins, the Calabria Wedge and the Mediterranean Ridge. In *Mémoire de la Société Géologique de France*, (Vol. 177, pp. 1–64). Paris: Société Géologique de France.

Channell, J. E. T. (1992). Paleomagnetic data from Umbria (Italy): Implications for the rotation of Adria and Mesozoic apparent polar wander paths. *Tectonophysics*, *216*(3–4), 365–378. https://doi.org/10.1016/0040-1951(92)90406-V

Channell, J. E. T. (1996). Palaeomagnetism and palaeogeography of Adria. In A. Morris, & D. H. Tarling (Eds.), *Palaeomagnetism and tectonics of the Mediterranean region*, *Special Publications*, (Vol. 105, pp. 119–132). London: Geological Society. https://doi.org/10.1144/GSL.SP.1996.105.01.01

Charier, S., Biju-Duval, B., Morel, Y., & Rossi, S. (1988). L'escarpement Apulien et le promontoire de Céphalonie: Marge septentrionale du bassin Ionien (synthèse des données des campagnes à la mer Escarmed). *Revue de l'Institut Français du Pétrole*, *43*(4), 485–515. https://doi.org/10.2516/ogst:1988030

Charier, S., Morel, Y., Biju-Duval, B., & Renard, V. (1987). L'Escarpement de Malte, le mont Alfeo et les monts de Médine: Marges anciennes du bassin Ionien (synthèse des données des campagnes à la mer Escarmed). *Revue de l'Institut Français Du Pétrole*, *42*(6), 695–745. https://doi.org/10.2516/ogst:1987041

Chaumillon, E., & Mascle, J. (1995). Variation laterale des fronts de deformation de la Ride mediterraneenne (Méditerranée orientale). *Bulletin de La Société Géologique de France*, *166*(5), 463–478. https://doi.org/10.2113/gssgfbull.166.5.463

Chaumillon, E., & Mascle, J. (1997). From foreland to forearc domains: New multichannel seismic reflection survey of the Mediterranean ridge accretionary complex (Eastern Mediterranean). *Marine Geology*, *138*(3–4), 237–259. https://doi.org/10.1016/S0025-3227(97)00002-9

Chaumillon, E., Mascle, J., & Hoffmann, H. J. (1996). Deformation of the western Mediterranean Ridge: Importance of Messinian evaporitic formations. *Tectonophysics*, *263*(1–4), 163–190. https://doi.org/10.1016/S0040-1951(96)00035-2

Ciarapica, G., & Passeri, L. (2002). The palaeogeographic duplicity of the Apennines. *Bollettino Della Società Geologica Italiana*, *121*(1), 67–75.

Collin, P.-Y., Mancinelli, A., Chiocchini, M., Mroueh, M., Hamdam, W., & Higazi, F. (2010). Middle and Upper Jurassic stratigraphy and sedimentary evolution of Lebanon (Levantine margin): Palaeoenvironmental and geodynamic implications. *Geological Society, London, Special Publications*, *341*(1), 227–244. https://doi.org/10.1144/SP341.11

Cowie, L., & Kusznir, N. (2012). Mapping crustal thickness and oceanic lithosphere distribution in the Eastern Mediterranean using gravity inversion. *Petroleum Geoscience*, *18*(4), 373–380. https://doi.org/10.1144/petgeo2011-071

Dannowski, A., Kopp, H., Klingelhoefer, F., Klaeschen, D., Gutscher, M.-A., Krabbenhoeft, A., et al. (2019). Ionian Abyssal Plain: A window into the Tethys oceanic lithosphere. *Solid Earth*, *10*(2), 447–462. https://doi.org/10.5194/se-10-447-2019

de Voogd, B., Truffert, C., Chamot-Rooke, N., Huchon, P., Lallemant, S., & Le Pichon, X. (1992). Two-ship deep seismic soundoings in the basins of the méditerranean sea (Pasiphae cruise). *Geophysical Journal International*, *109*(3), 536–552. https://doi.org/10.1111/j.1365-246X.1992.tb00116.x

Dean, S. M., Minshull, T. A., Whitmarsh, R. B., & Louden, K. E. (2000). Deep structure of the ocean-continent transition in the southern Iberia Abyssal Plain from seismic refraction profiles: The IAM-9 transect at 40, 20N. *Journal of Geophysical Research*, *105*(B3), 5859–5885 . https://doi.org/10.1029/1999JB900301

Del Ben, A., & Finetti, I. (1991). Geophysical study of the Sirt Rise. In *Symposium on the Geology of Libya, 3*, (Vol. VI, pp. 2417–2431. Retrieved from). http://search.ebscohost.com/login.aspx?direct=true&db=geh&AN=1994-027764&lang=fr&site=eds-live

Del Ben, A., Mocnik, A., Volpi, V., & Karvelis, P. (2015). Old domains in the South Adria plate and their relationship with the West Hellenic front. *Journal of Geodynamics*, *89*, 15–28. https://doi.org/10.1016/j.jog.2015.06.003

Delescluse, M., Funck, T., Dehler, S. A., Louden, K. E., & Watremez, L. (2015). The oceanic crustal structure at the extinct, slow to ultraslow Labrador Sea spreading center. *Journal of Geophysical Research: Solid Earth*, *120*, 5249–5272. https://doi.org/10.1002/2014JB011739

Dellong, D., Klingelhoefer, F., Kopp, H., Graindorge, D., Margheriti, L., Moretti, M., et al. (2018). Crustal structure of the Ionian Basin and Eastern Sicily Margin: Results from a wide-angle seismic survey. *Journal of Geophysical Research: Solid Earth*, *123*(3), 2090–2114. https://doi.org/10.1002/2017JB015312

Dercourt, J., Ricou, L. E., & Vrielynck, B. (1993). *Atlas Tethys of paleoenvironmental maps*. Paris: Gauthier-Villars.

Dercourt, J., Zonenshain, L. P., Ricou, L. E., Kazmin, V. G., Le Pichon, X., Knipper, A. L., et al. (1986). Geological evolution of the Tethys belt from the Atlantic to the Pamirs since the Lias. *Tectonophysics*, *123*(1–4), 241–315. https://doi.org/10.1016/0040-1951(86)90199-x

Duronio, P., Dakshi, A., Bellini, E., & Dakshe, A. (1991). Stratigraphy of the offshore Cyrenaica (Libya). In *The Geology of Libya*, (Vol. IV, pp. 1589–1620). Amsterdam: Elsevier.

Emeis, K.-C., Robertson, A. H. F., Richter, C., et al., (1996). Proc. ODP, Init. Repts., 160: College Station, TX: Ocean Drilling Program. https://doi.org/10.2973/odp.proc.ir.160.1996

Enay, R., Bizon, J. J., Mascle, G., Morel, Y., & Perrier, R. (1982). Faunes du Jurassique supérieur dans les séries pélagiques de l'escarpement de Malte (Mer Ionienne). Implications paléogéographiques. *Revue de l'Institut Français Du Pétrole*, *37*(6), 733–757. https://doi.org/10.2516/ogst:1982037

Fabricius, F., & Hieke, W. (1977). Neogene to Quaternary development of the Ionian Basin (Mediterranean): Considerations based on a "dynamic shallow basin model" of the Messinian salinity event. In *Structural history of the Mediterranean Basins*, (pp. 391–400). Paris: Technip, Editions.

Fabricius, F. H. (1984). Neogene to Quaternary geodynamics of the area of the Ionian Sea and surrounding land masses. *Geological Society, London, Special Publications*, *17*(1), 819–824. https://doi.org/10.1144/GSL.SP.1984.017.01.67

Faccenna, C., Jolivet, L., Piromallo, C., & Morelli, A. (2003). Subduction and the depth of convection in the Mediterranean mantle. *Journal of Geophysical Research*, *108*(B2), 2099. https://doi.org/10.1029/2001JB001690

Ferruci, F., Gaudiosi, G., Hirn, A., & Nicolich, R. (1991). Ionian Basin and Calabria Arc: Some new elements from DSS data. *Tectonophysics*, *195*(2-4), 411–419. https://doi.org/10.1016/0040-1951(91)90223-f

Finetti, I. (1982). Structure, Stratigraphy and evolution of central Mediterranean. *Bollettino di Geofisica Teorica ed Applicata*, *24*(96), 247–312. https://doi.org/10.1007/s10539-010-9244-0

Finetti, I., & Morelli, C. (1972). Wide scale digital seismic exploration of the Mediterranean Sea. *Bollettino di Geofisica Teorica ed Applicata*, *14*(56), 291–342.

Finetti, I. R. (Ed) (2005). *CROP project: Deep seismic exploration of the central Mediterranean and Italy, CROP PROJECT*, (Vol. 1). Amsterdam, Boston: Elsevier.

Finetti, I. R., & Del Ben, A. (2005). Crustal tectono-stratigraphy of the Ionian Sea from new integrated CROP seismic data. In *Deep Seismic Exploration of the Central Mediterranean and Italy, CROP PROJECT*, (Vol. 19, pp. 447–470). Amsterdam, Boston: Elsevier.

Frizon de Lamotte, D., Fourdan, B., Leleu, S., Leparmentier, F., & de Clarens, P. (2015). Style of rifting and the stages of Pangea breakup. *Tectonics*, *34*, 1009–1029. https://doi.org/10.1002/2014TC003760

Frizon de Lamotte, D., Raulin, C., Mouchot, N., Wrobel-Daveau, J.-C., Blanpied, C., & Ringenbach, J.-C. (2011). The southernmost margin of the Tethys realm during the Mesozoic and Cenozoic: Initial geometry and timing of the inversion processes. *Tectonics*, *30*, TC3002. https://doi.org/10.1029/2010TC002691

Frizon de Lamotte, D., Tavakoli-Shirazi, S., Leturmy, P., Averbuch, O., Mouchot, N., Raulin, C., et al. (2013). Evidence for Late Devonian vertical movements and extensional deformation in northern Africa and Arabia: Integration in the geodynamics of the Devonian world. *Tectonics*, *32*, 107–122. https://doi.org/10.1002/tect.20007

Gabtni, H., Jallouli, C., Mickus, K. L., & Turki, M. M. (2013). Geodynamics of the Southern Tethyan Margin in Tunisia and Maghrebian domain: New constraints from integrated geophysical study. *Arabian Journal of Geosciences*, *6*(1), 271–286. https://doi.org/10.1007/s12517-011-0362-z

Gallais, F., Graindorge, D., Gutscher, M.-A., & Klaeschen, D. (2013). Propagation of a lithospheric tear fault (STEP) through the western boundary of the Calabrian accretionary wedge offshore eastern Sicily (Southern Italy). *Tectonophysics*, *602*, 141–152. https://doi.org/10.1016/j.tecto.2012.12.026

Gallais, F., Gutscher, M. A., Graindorge, D., Chamot-Rooke, N., & Klaeschen, D. (2011). A Miocene tectonic inversion in the Ionian Sea (central Mediterranean): Evidence from multichannel seismic data. *Journal of Geophysical Research*, *116*, B12108. https://doi.org/10.1029/2011JB008505

Gallais, F., Gutscher, M. A., Klaeschen, D., & Graindorge, D. (2012). Two-stage growth of the Calabrian accretionary wedge in the Ionian Sea (Central Mediterranean): Constraints from depth-migrated multichannel seismic data. *Marine Geology*, *326-328*, 28–45. https://doi.org/10.1016/j.margeo.2012.08.006

Gardosh, M. A., & Druckman, Y. (2006). Seismic stratigraphy, structure and tectonic evolution of the Levantine Basin, offshore Israel. *Geological Society, London, Special Publications*, *260*(1), 201–227. https://doi.org/10.1144/GSL.SP.2006.260.01.09

Gardosh, M. A., Garfunkel, Z., Druckman, Y., & Buchbinder, B. (2010). Tethyan rifting in the Levant Region and its role in Early Mesozoic crustal evolution. *Geological Society, London, Special Publications*, *341*(1), 9–36. https://doi.org/10.1144/SP341.2

Garfunkel, Z. (1998). Constrains on the origin and history of the Eastern Mediterranean basin. *Tectonophysics*, *298*(1–3), 5–35. https://doi.org/10.1016/S0040-1951(98)00176-0

Garfunkel, Z. (2004). Origin of the Eastern Mediterranean basin: A reevaluation. *Tectonophysics*, *391*(1–4), 11–34. https://doi.org/10.1016/j.tecto.2004.07.006

Garfunkel, Z., & Derin, B. (1984). Permian-early Mesozoic tectonism and continental margin formation in Israel and its implications for the history of the Eastern Mediterranean. *Geological Society, London, Special Publications*, *17*(1), 187–201. https://doi.org/10.1144/GSL.SP.1984.017.01.12

Giese, P., Reutter, K. J., Jacobshagen, V., & Nicolich, R. (1982). Explosion seismic crustal studies in the Alpine Mediterranean region and their implications to tectonic processes. In H. Berckhemer, & K. Hsü (Eds.), *Alpine-Mediterranean geodynamics*, *Geodynamics Series*, (Vol. 7, pp. 39–73). American Geophysical Union. https://doi.org/10.1029/GD007p0039

Gradstein, F., & Ogg, J. (2004). Geologic Time Scale 2004—Why, how, and where next! *Lethaia*, *37*(2), 175–181. https://doi.org/10.1080/00241160410006483

Granot, R. (2016). Palaeozoic oceanic crust preserved beneath the eastern Mediterranean. *Nature Geoscience*, *9*(9), 701–705. https://doi.org/10.1038/ngeo2784

Grevemeyer, I., Ranero, C. R., & Ivandic, M. (2018). Structure of oceanic crust and serpentinization at subduction trenches. *Geosphere*, *14*(2), 395–418. https://doi.org/10.1130/GES01537.1

Groupe-Escarmed, Charier, S., Burollet, P. F., Morel, Y., & Biju-Duval, B. (1987). Le plateau Cyrénien: Promontoire africain sur la marge Ionienne. *Revue de l'Institut Français du Pétrole*, *42*(4), 419–447. https://doi.org/10.2516/ogst:1987025

Guiraud, R., Bosworth, W., Thierry, J., & Delplanque, A. (2005). Phanerozoic geological evolution of Northern and Central Africa: An overview. *Journal of African Earth Sciences*, *43*(1-3), 83–143. https://doi.org/10.1016/j.jafrearsci.2005.07.017

Gutscher, M. A., Kopp, H., Krastel, S., Bohrmann, G., Garlan, T., Zaragosi, S., et al. (2017). Active tectonics of the Calabrian subduction revealed by new multi-beam bathymetric data and high-resolution seismic profiles in the Ionian Sea (Central Mediterranean). *Earth and Planetary Science Letters*, *461*, 61–72. https://doi.org/10.1016/j.epsl.2016.12.020

Hairabian, A., Fournier, F., Borgomano, J., & Nardon, S. (2014). Depositional facies, pore types and elastic properties of deep-water gravity flow carbonates. *Journal of Petroleum Geology*, *37*(3), 231–249. https://doi.org/10.1111/jpg.12581

Handy, M. R., Schmid, S. M., Bousquet, R., Kissling, E., & Bernoulli, D. (2010). Reconciling plate-tectonic reconstructions of Alpine Tethys with the geological—Geophysical record of spreading and subduction in the Alps. *Earth Science Reviews*, *102*(3–4), 121–158. https://doi.org/10.1016/j.earscirev.2010.06.002

Hawie, N., Gorini, C., Deschamps, R., Nader, F. H., Montadert, L., Granjeon, D., & Baudin, F. (2013). Tectono-stratigraphic evolution of the northern Levant Basin (offshore Lebanon). *Marine and Petroleum Geology*, *48*, 392–410. https://doi.org/10.1016/j.marpetgeo.2013.08.004

Hieke, W., Camerlenghi, A., Cita, M. B., Dehghani, G. A., Fusi, N., Hirschleber, H. B., et al. (2009). Bannock Basin, Sirte Abyssal Plain and Conrad Spur: Structural relationships between Mediterranean Ridge and its western foreland and implications on the character of the accretionary complex (eastern Mediterranean). *Marine Geophysical Researches*, *30*(3), 161–192. https://doi.org/10.1007/s11001-009-9075-z

Hieke, W., Hirschleber, H. B., & Dehghani, G. A. (1998). The crust of the Ionian Abyssal Plain—Old oceanic ? *Rapports de la Commission Internationale pour l'exploration scientifique de la mer Méditerranée*, *35*, 72–73.

Hieke, W., Hirschleber, H. B., & Dehghani, G. A. (2003). The Ionian Abyssal Plain (central Mediterranean Sea): Morphology, subbottom structures and geodynamic history—An inventory. *Marine Geophysical Researches*, *24*(3–4), 279–310. https://doi.org/10.1007/s11001-004-2173-z

Hinz, K. (1974). Results of seismic refraction and seismic reflection measurements in the Ionian Sea. *Geologiches Jahrbuch, Reihe Geophysik*, *2*, 33–65.

Hirn, A., Nicolich, R., Gallart, J., Laigle, M., Cernobori, L., & ETNASEIS Scientific Group (1997). Roots of Etna volcano in faults of great earthquakes. *Earth and Planetary Science Letters*, *148*(1-2), 171–191.

Homberg, C., Barrier, E., Mroueh, M., Muller, C., Hamdan, W., & Higazi, F. (2010). Tectonic evolution of the central Levant domain (Lebanon) since Mesozoic time. *Geological Society, London, Special Publications*, *341*(1), 245–268. https://doi.org/10.1144/SP341.12

Hsu, K., & Montadert, L. (1978). *Initial reports of the Deep Sea Drilling Project*, (Vol. 42 Pt. 1). Washington, D.C.: U.S. Government Printing Office. https://doi.org/10.2973/dsdp.proc.42-1.1978

Hsu, K., Montadert, L., Bernoulli, D., Bizon, G., Cita, M., Erickson, A., et al. (1978). *Site 374: Messina Abyssal Plain. In Initial reports of the Deep Sea Drilling Project*, (Vol. *42* Pt. 1). Washington, D.C.: U.S. Government Printing Office. https://doi.org/10.2973/dsdp.proc.42-1.105.1978

Jolivet, J., Augier, R., Faccenna, C., Negro, F., Rimmele, G., Agard, P., et al. (2008). Subduction, convergence and the mode of backarc extension in the Mediterranean region. *Bulletin de la Société Géologique de France*, *179*(6), 525–550. https://doi.org/10.2113/gssgfbull.179.6.525

Jolivet, L., & Brun, J.-P. (2010). Cenozoic geodynamic evolution of the Aegean. *International Journal of Earth Sciences Geologische Rundschau*, *99*(1), 109–138. https://doi.org/10.1007/s00531-008-0366-4

Jolivet, L., Faccenna, C., Agard, P., Frizon de Lamotte, D., Menant, A., Sternai, P., & Guillocheau, F. (2015). Neo-Tethys geodynamics and mantle convection: From extension to compression in Africa and a conceptual model for obduction. *Canadian Journal of Earth Sciences*, *53*(11), 1190–1204. https://doi.org/10.1139/cjes-2015-0118

Jones, K. A., Warner, M., Le Meur, D., Pascal, G., & Tay, P. L. (2002). Wide-angle images of the Mediterranean Ridge backstop structure. *Marine Geology*, *186*(1–2), 145–166. https://doi.org/10.1016/S0025-3227(02)00177-9

Jongsma, D., van Hinte, J. E., & Woodside, J. M. (1985). Geologic structure and neotectonics of the North African Continental margin south of Sicily. *Marine and Petroleum Geology*, *2*(2), 156–179. https://doi.org/10.1016/0264-8172(85)90005-4

Keeley, M. L., & Massoud, M. S. (1998). Tectonic controls on the petroleum geology of NE Africa. *Geological Society, London, Special Publications*, *132*(1), 265–281. https://doi.org/10.1144/GSL.SP.1998.132.01.15

Kent, D. V., & Olsen, P. E. (1999). Astronomically tuned geomagnetic polarity timescale for the Late Triassic. *Journal of Geophysical Research*, *104*(B6), 12,831–12,841. https://doi.org/10.1029/1999JB900076

Kent, D. V., & Olsen, P. E. (2008). Early Jurassic magnetostratigraphy and paleolatitudes from the Hartford continental rift basin (eastern North America): Testing for polarity bias and abrupt polar wander in association with the central Atlantic magmatic province. *Journal of Geophysical Research*, *113*(B6), B06105. https://doi.org/10.1029/2007JB005407

Kioka, A., Ashi, J., Sakaguchi, A., Sato, T., Muraoka, S., Yamaguchi, A., et al. (2015). Possible mechanism of mud volcanism at the prism-backstop contact in the western Mediterranean Ridge Accretionary Complex. *Marine Geology*, *363*, 52–64. https://doi.org/10.1016/j.margeo.2015.01.014

Labails, C., Olivet, J. L., Aslanian, D., & Roest, W. R. (2010). An alternative early opening scenario for the Central Atlantic Ocean. *Earth and Planetary Science Letters*, *297*(3–4), 355–368. https://doi.org/10.1016/j.epsl.2010.06.024

Lallemant, S., Truffert, C., Jolivet, L., Henry, P., Chamot-Rooke, N., & de Voogd, B. (1994). Spatial transition from compression to extension in the Western Mediterranean Ridge accretionary complex. *Tectonophysics*, *234*(1–2), 33–52. https://doi.org/10.1016/0040-1951(94)90203-8

Le Breton, E., Handy, M. R., Molli, G., & Ustaszewski, K. (2017). Post-20 Ma motion of the Adriatic Plate: New constraints from surrounding orogens and implications for crust-mantle decoupling. *Tectonics*, *36*, 3135–3154. https://doi.org/10.1002/2016TC004443

Le Meur, D. (1997). Etude géophysique de la structure profonde et de la tectonique active de la partie occidentale de Ride Méditerranéenne, 225pp., PhD thesis, Univ. Paris XI, Paris.

Le Pichon, X., Şengör, C., & İmren, C. (2019). A new approach to the opening of the Eastern Mediterranean Sea and the origin of the Hellenic Subduction Zone—Part 1: The Eastern Mediterranean Sea. *Canadian Journal of Earth Sciences*. https://doi.org/10.1139/cjes-2018-0128

Leprêtre, R., Frizon de Lamotte, D., Combier, V., Gimeno-Vives, O., Mohn, G., & Eschard, R. (2018). The Tell-Rif orogenic system (Morocco, Algeria, Tunisia) and the structural heritage of the southern Tethys margin. *BSGF - Earth Sciences Bulletin*, *189*(2), 10. https://doi.org/10.1051/bsgf/2018009

Leroy, M., Gueydan, F., & Dauteuil, O. (2008). Uplift and strength evolution of passive margins inferred from 2-D conductive modelling. *Geophysical Journal International*, *172*(1), 464–476. https://doi.org/10.1111/j.1365-246X.2007.03566.x

Lipparini, L., Scrocca, D., Marsili, P., & Morandi, S. (2009). Offshore Malta licence in the Central Mediterranean Sea offers hope of hydrocarbon potential. *First Break*, *27*(2), 105–116.

Lofi, J., Déverchère, J., Gaullier, V., Gillet, H., Gorini, C., Guennoc, P., et al. (2011). Seismic atlas of the Messinian Salinity Crisis markers in the Mediterranean and Black Seas. In *Mémoires de la Société Géologique de France*, (Vol. *179*, p. 72). Commission for the Geological Map of the World (CGMW)/Société Géologique de France: Paris.

Makris, J., Abraham, Z. B., Behle, A., Ginzburg, A., Giese, P., Steinmetz, L., et al. (1983). Seismic refraction profiles between Cyprus and Israel and their interpretation. *Geophysical Journal of the Royal Astronomical Society*, *75*(3), 575–591. https://doi.org/10.1111/j.1365-246X.1983.tb05000.x

Makris, J., Nicolich, R., & Weigel, W. (1986). A seismic study in the Western Ionian Sea. *Annales Geophysicae*, *4*(6), 665–678.

Malinverno, A., & Ryan, W. B. F. (1986). Extension in the Tyrrhenian Sea and shortening in the Apennines as result of arc migration driven by sinking of the lithosphere. *Tectonics*, *5*(2), 227–245. https://doi.org/10.1029/TC005i002p00227

Martin, M., Starkie, S., Yanilmaz, E., Huffman, D. P., Gutteridge, P., Coles, G., et al. (2008). Sequence stratigraphy of the Precambrian to Middle Miocene of NE Libya. In M. J. Salem, & A. S. El Hawat (Eds.), *Third Symposium on the Sedimentary Basin of Libya, Geology of East Libya*, (Vol. *1*, pp. 263–294). Tripoli: Earth Science Society of Libya.

Massa, D., & Delort, T. (1984). Evolution du bassin de Syrte (Libye) du Cambrien au Crétacé basal. *Bulletin de La Societé Géologique de France*, *7*(6), 1087–1096.

Mejri, F., Burollet, P. F., & Ben Ferjani, A. (2006). Petroleum geology of Tunisia: A renewed synthesis. *Entrep Tunis Activ Petrol, Memoir*, *22*.

Minelli, L., & Faccenna, C. (2010). Evolution of the Calabrian accretionary wedge (central Mediterranean). *Tectonics*, *29*, TC4004. https://doi.org/10.1029/2009TC002562

Mohn, G., Manatschal, G., Müntener, O., Beltrando, M., & Masini, E. (2010). Unravelling the interaction between tectonic and sedimentary processes during lithospheric thinning in the Alpine Tethys margins. *International Journal of Earth Sciences*, *99*(S1), 75–101. https://doi.org/10.1007/s00531-010-0566-6

Montadert, L., Nicolaides, S., Semb, P. H., & Lie, Ø. (2014). Petroleum systems offshore Cyprus. In L. Marlow, C. Kendall, & L. Yose (Eds.), *Petroleum Systems of the Tethyan Region*, (Vol. 106, pp. 301–334). AAPG Memoir.

Moustafa, A. R. (2008). Mesozoic-Cenozoic Basin evolution in the northern western desert of Egypt. In M. Salem, A. El-Arnauti, & A. Saleh (Eds.), *The Geology of East Libya*, (Vol. 3, pp. 29–46). MaltaName of the publisher: Gutenberg Press Ltd.

Muller, M. R., Robinson, C. J., Minshull, T. A., White, R. S., & Bickle, M. J. (1997). Thin crust beneath ocean drilling program borehole 735B at the Southwest Indian Ridge? *Earth and Planetary Science Letters*, *148*(1–2), 93–107. https://doi.org/10.1016/S0012-821X(97)00030-7

Muttoni, G., Dallanave, E., & Channell, J. E. T. (2013). The drift history of Adria and Africa from 280 Ma to Present, Jurassic true polar wander, and zonal climate control on Tethyan sedimentary facies. *Palaeogeography, Palaeoclimatology, Palaeoecology*, *386*, 415–435. https://doi.org/10.1016/j.palaeo.2013.06.011

Muttoni, G., Kent, D. V., & Channell, J. E. T. (1996). Evolution of Pangea: Paleomagnetic constraints from the Southern Alps, Italy. *Earth and Planetary Science Letters*, *140*(1–4), 97–112. https://doi.org/10.1016/0012-821X(96)00038-6

Muttoni, G., Kent, D. V., Garzanti, E., Brack, P., Abrahamsen, N., & Gaetani, M. (2003). Early Permian Pangea "B" to Late Permian Pangea "A.". *Earth and Planetary Science Letters*, *215*(3-4), 379–394. https://doi.org/10.1016/S0012-821X(03)00452-7

Naliboff, J., & Buiter, S. J. H. (2015). Rift reactivation and migration during multiphase extension. *Earth and Planetary Science Letters*, *421*, 58–67. https://doi.org/10.1016/j.epsl.2015.03.050

Netzeband, G. L., Gohl, K., Hübscher, C. P., Ben-Avraham, Z., Dehghani, G. A., Gajewski, D., & Liersch, P. (2006). The Levantine Basin—Crustal structure and origin. *Tectonophysics*, *418*(3–4), 167–188. https://doi.org/10.1016/j.tecto.2006.01.001

Nicolich, R., Laigle, M., Hirn, A., Cernobori, L., & Gallart, J. (2000). Crustal structure of the Ionian margin of Sicily: Etna volcano in the frame of regional evolution. *Tectonophysics*, *329*(1–4), 121–139. https://doi.org/10.1016/S0040-1951(00)00192-X

Pagot, P., Chamot-Rooke, N., Lallemant, S., Pascal, G., Dessa, J.-X., Le Pichon, X., et al. (1999). Compressional deformation in the Ionian basin: New seismic data. European Geophysical Society, XXIV General Assembly, The Hague, The Netherlands, April 19-23 1999.

Parsons, B., & Sclater, J. G. (1977). An analysis of the variation of ocean floor bathymetry and heat flow with age. *Journal of Geophysical Research*, *82*(5), 803–827. https://doi.org/10.1029/JB082i005p00803

Pascal, G. (1997). ARCHIMEDE cruise, *RV Le Nadir*, https://doi.org/10.17600/97080020

Patacca, E., Scandone, P., & Giunta, G. (1979). Mesozoic paleotectonic evolution of the Ragusa zone (Southeastern Sicily). *Geologica Romana*, *18*, 331–369.

Polonia, A., Bonatti, E., Camerlenghi, A., Lucchi, R. G., Panieri, G., & Gasperini, L. (2013). Mediterranean megaturbidite triggered by the AD 365 Crete earthquake and tsunami. *Scientific Reports*, *3*(1), 1285. https://doi.org/10.1038/srep01285

Polonia, A., Camerlenghi, A., Davey, F., & Storti, F. (2002). Accretion, structural style and syn-contractional sedimentation in the Eastern Mediterranean Sea. *Marine Geology*, *186*(1–2), 127–144. https://doi.org/10.1016/S0025-3227(02)00176-7

Polonia, A., Torelli, L., Artoni, A., Carlini, M., Faccenna, C., Ferranti, L., et al. (2016). The Ionian and Alfeo–Etna fault zones: New segments of an evolving plate boundary in the central Mediterranean Sea? *Tectonophysics*, *675*, 69–90. https://doi.org/10.1016/j.tecto.2016.03.016

Polonia, A., Torelli, L., Gasperini, L., Cocchi, L., Muccini, F., Bonatti, E., et al. (2017). Lower plate serpentinite diapirism in the Calabrian Arc subduction complex. *Nature Communications*, *8*(1), 2172. https://doi.org/10.1038/s41467-017-02273-x

Polonia, A., Torelli, L., Mussoni, P., Gasperini, L., Artoni, A., & Klaeschen, D. (2011). The Calabrian Arc subduction complex in the Ionian Sea: Regional architecture, active deformation, and seismic hazard. *Tectonics*, *30*, TC5018. https://doi.org/10.1029/2010TC002821

Prada, M., Sallares, V., Ranero, C. R., Vendrell, M. G., Grevemeyer, I., Zitellini, N., & de Franco, R. (2015). The complex 3-D transition from continental crust to backarc magmatism and exhumed mantle in the Central Tyrrhenian basin. *Geophysical Journal International*, *203*(1), 63–78. https://doi.org/10.1093/gji/ggv271

QGIS Development Team (2015). QGIS Geographic Information System. Open Source Geospatial Foundation Project. http://qgis.osgeo.org

Rabaute, A., & Chamot-Rooke, N. (2007). Quantitative mapping of active mud volcanism at the western Mediterranean Ridge-backstop contact. *Marine Geophysical Researches*, *28*(3), 271–295. https://doi.org/10.1007/s11001-007-9031-8

Raulin, C., Frizon de Lamotte, D., Bouaziz, S., Khomsi, S., Mouchot, N., Ruiz, G., & Guillocheau, F. (2011). Late Triassic–early Jurassic block tilting along E–W faults, in southern Tunisia: New interpretation of the Tebaga of Medenine. *Journal of African Earth Sciences*, *61*(1), 94–104. https://doi.org/10.1016/j.jafrearsci.2011.05.007

Reston, T., Fruehn, J., & von Huene, R. (2002). The structure and evolution of the western Mediterranean Ridge. *Marine Geology*, *186*(1–2), 83–110. https://doi.org/10.1016/S0025-3227(02)00174-3

Reston, T. J., Von Huene, R., Dickmann, T., Klaeschen, D., & Kopp, H. (2002). Frontal accretion along the western Mediterranean Ridge: The effect of Messinian evaporites on wedge mechanics and structural style. *Marine Geology*, *186*(1-2), 59–82. https://doi.org/10.1016/S0025-3227(02)00173-1

Robertson, A. H. F. (2006). Sedimentary evidence from the south Mediterranean region (Sicily, Crete, Peloponnese, Evia) used to test alternative models for the regional tectonic setting of Tethys during Late Palaeozoic-Early Mesozoic time. *Geological Society, London, Special Publications*, *260*(1), 91–154. https://doi.org/10.1144/GSL.SP.2006.260.01.06

Robertson, A. H. F. (2007). Overview of tectonic settings related to the rifting and opening of Mesozoic ocean basins in the Eastern Tethys: Oman, Himalayas and Eastern Mediterranean regions. *Geological Society, London, Special Publications*, *282*(1), 325–388. https://doi.org/10.1144/SP282.15

Robertson, A. H. F., Dixon, J. E., Brown, S., Collins, A., Morris, A., Pickett, E., et al. (1996). Alternative tectonic models for the Late Palaeozoic-Early Tertiary development of Tethys in the Eastern Mediterranean region. *Geological Society, London, Special Publications*, *105*(1), 239–263. https://doi.org/10.1144/GSL.SP.1996.105.01.22

Rosenbaum, G., Lister, G. S., & Duboz, C. (2004). The Mesozoic and Cenozoic motion of Adria (central Mediterranean): A review of constraints and limitations. *Geodinamica Acta*, *17*(2), 125–139. https://doi.org/10.3166/ga.17.125-139

Rossi, S., & Borsetti, A. M. (1977). Dati preliminari di stratigrafia e di sismica del Mare Ionio settentrionale. *Memorie della Societa Geologica Italiana*, *13*, 251–259.

Roure, F., Casero, P., & Addoum, B. (2012). Alpine inversion of the North African margin and delamination of its continental lithosphere. *Tectonics*, *31*, TC30006. https://doi.org/10.1029/2011TC002989

Ryan, W. B. F., & Hsu, K. J. (1973). *Initial reports of the Deep Sea Drilling Project*, (Vol. 13). U.S. Government Printing Office. https://doi.org/10.2973/dsdp.proc.13.1973

Ryan, W. B. F., Kastens, K. A., & Cita, M. B. (1982). Geological evidence concerning compressional tectonics in the eastern Mediterranean. *Tectonophysics*, *86*(1–3), 213–242. https://doi.org/10.1016/0040-1951(82)90068-3

Sandwell, D. T., Müller, R. D., Smith, W. H. F., Garcia, E., & Francis, R. (2014). New global marine gravity model from CryoSat-2 and Jason-1 reveals buried tectonic structure. *Science (New York, N.Y.)*, *346*(6205), 65–67. https://doi.org/10.1126/science.1258213

Santantonio, M., Scrocca, D., & Lipparini, L. (2013). The Ombrina-Rospo Plateau (Apulian Platform): Evolution of a Carbonate Platform and its Margins during the Jurassic and Cretaceous. *Marine and Petroleum Geology*, *42*, 4–29. https://doi.org/10.1016/j.marpetgeo.2012.11.008

Scandone, P., Patacca, E., Radoicic, R., Ryan, W. B. F., Cita, M. B., Rawson, M., et al. (1981). Mesozoic and Cenozoic rocks from Maltal Escarpment (Central Mediterranean). *AAPG Bulletin*, *65*(7), 1299–1319. https://doi.org/10.1306/03B5949F-16D1-11D7-8645000102C1865D

Schettino, A., & Turco, E. (2011). Tectonic history of the western Tethys since the Late Triassic. *Geological Society of America Bulletin*, *123*(1–2), 89–105. https://doi.org/10.1130/B30064.1

Scrocca, D. (2010). Southern apennines: Structural setting and tectonic evolution. *Journal of the Virtual Explorer*, *36*, 1–23. https://doi.org/10.3809/jvirtex.2010.00225

Segev, A., Sass, E., & Schattner, U. (2018). Age and structure of the Levant basin, Eastern Mediterranean. *Earth-Science Reviews*, *182*, 233–250. https://doi.org/10.1016/j.earscirev.2018.05.011

Şengör, A. M. C. (1979). Mid-Mesozoic closure of Permo–Triassic Tethys and its implications. *Nature*, *279*(5714), 590–593. https://doi.org/10.1038/279590a0

Şengör, A. M. C., Yilmaz, Y., & Sungurlu, O. (1984). Tectonics of the Mediterranean Cimmerides: Nature and evolution of the western termination of Palaeo-Tethys. *Geological Society, London, Special Publications*, *17*(1), 77–112. https://doi.org/10.1144/GSL.SP.1984.017.01.04

Sioni, S. (1996). Mer Ionienne et Apulie depuis l'ouverture de l'Océan Alpin. 241 pp., Ph.D. thesis, Université de Bretagne Occidentale, Brest, France.

Speranza, F., Minelli, L., Pignatelli, A., & Chiappini, M. (2012). The Ionian Sea: The oldest in situ ocean fragment of the world? *Journal of Geophysical Research*, *117*, B12101. https://doi.org/10.1029/2012JB009475

Stampfli, G., Marcoux, J., & Baud, A. (1991). Tethyan margins in space and time. *Palaeogeography, Palaeoclimatology, Palaeoecology*, *87*(1–4), 373–409. https://doi.org/10.1016/0031-0182(91)90142-E

Stampfli, G. M., & Borel, G. D. (2002). A plate tectonic model for the Paleozoic and Mesozoic constrained by dynamic plate boundaries and restored synthetic oceanic isochrons. *Earth and Planetary Science Letters*, *196*(1–2), 17–33. https://doi.org/10.1016/S0012-821X(01)00588-X

Stampfli, G. M., Mosar, J., Favre, P., Pillevuit, A., & Vannay, J.-C. (2001). Permo-Mesozoic evolution of the western Tethys realm: The Neo-Tethys East Mediterranean Basin connection. In A. Ziegler, W. Cavazza, A. H. F. Robertson, & S. Carasquin-Soleau (Eds.), *Peri-Tethys memoir 6; Peri-Tethyan rift/wrench basins and passive margins*, (Vol. 186, pp. 51–108). Paris: Mémoires du Muséum national d'histoire naturelle.

Steckler, M. S., & ten Brink, U. S. (1986). Lithospheric strength variations as a control on new plate boundaries: Examples from the northern Red Sea region. *Earth and Planetary Science Letters*, *79*(1-2), 120–132. https://doi.org/10.1016/0012-821X(86)90045-2

Stein, C. A., & Stein, S. (1992). A model for the global variation in oceanic depth and heat flow with lithospheric age. *Nature*, *359*(6391), 123–129. https://doi.org/10.1038/359123a0

Steinberg, J., Roberts, A. M., Kusznir, N. J., Schafer, K., & Karcz, Z. (2018). Crustal structure and post-rift evolution of the Levant Basin. *Marine and Petroleum Geology*, *96*, 522–543. https://doi.org/10.1016/j.marpetgeo.2018.05.006

Tari, G., Kohazy, R., Hannke, K., Hussein, H., Novotny, B., & Mascle, J. (2012). Examples of deep-water play types in the Matruh and Herodotus basins of NW Egypt. *The Leading Edge*, *31*(7), 816–823. https://doi.org/10.1190/tle31070816.1

Tassy, A., Crouzy, E., Gorini, C., Rubino, J.-L., Bouroullec, J.-L., & Sapin, F. (2015). Egyptian Tethyan margin in the Mesozoic: Evolution of a mixed carbonate-siliciclastic shelf edge (from Western Desert to Sinai). *Marine and Petroleum Geology*, *68*, 565–581. https://doi.org/10.1016/j.marpetgeo.2015.10.011

Thusu, B. (1996). Implication of the discovery of reworked and in situ late palaeozoic and triassic playnomorphs on the evolution of Sirt basin, Libya. In M. Salem, M. Mouzughi, & O. Hammuda (Eds.), *The Geology of Sirt Basin*, (pp. 455–474). Amsterdam, Netherlands: Elsevier.

Truffert, C., Chamot-Rooke, N., Lallemant, S., Voogd, B., Huchon, P., & Pichon, X. (1993). The crust of the Western Mediterranean Ridge from deep seismic data and gravity modelling. *Geophysical Journal International*, *114*(2), 360–372. https://doi.org/10.1111/j.1365-246X.1993.tb03924.x

Vai, G. B. (2003). Development of the palaeogeography of Pangaea from Late Carboniferous to Early Permian. *Palaeogeography, Palaeoclimatology, Palaeoecology*, *196*(1–2), 125–155. https://doi.org/10.1016/S0031-0182(03)00316-X

Van Hinsbergen, D. J. J., Mensink, M., Langereis, C. G., Maffione, M., Spalluto, L., Tropeano, M., & Sabato, L. (2014). Did Adria rotate relative to Africa? *Solid Earth*, *5*(2), 611–629. https://doi.org/10.5194/se-5-611-2014

VIDEPI Project (2016). Visibility of Petroleum Exploration Data in Italy. http://unmig.sviluppoeconomico.gov.it/videpi/en/pozzi/pozzi.asp

Vlahović, I., Tišljar, J., Velić, I., & Matičec, D. (2005). Evolution of the Adriatic Carbonate Platform: Palaeogeography, main events and depositional dynamics. *Palaeogeography, Palaeoclimatology, Palaeoecology*, *220*(3–4), 333–360. https://doi.org/10.1016/j.palaeo.2005.01.011

Wennekers, J. H. N., Wallace, F. K., & Abugares, Y. I. (1996). The geology and hydrocarbons of the Sirt basin. In *The Geology of Sirt Basin*, (Vol. 1, pp. 3–56). Amsterdam: Elsevier.

Wessel, P., Smith, W. H. F., Scharroo, R., Luis, J., & Wobbe, F. (2013). Generic Mapping Tools: Improved version released. *Eos, Transactions American Geophysical Union*, *94*(45), 409–410. https://doi.org/10.1002/2013EO450001

White, R. S., McKenzie, D., & O'Nions, R. K. (1992). Oceanic crustal thickness from seismic measurements and rare earth element inversions. *Journal of Geophysical Research*, *97*(B13), 19683. https://doi.org/10.1029/92JB01749

Yanilmaz, E., Huffman, D., Martin, M., & Gutteridge, P. (2008). Facies analysis and depositional systems of defined sedimentary sequences from Precambrian to Late Miocene in NE Libya. In *Geology of East Libya*, (Vol. 1, pp. 3–84).

Yellin-Dror, A., Grasso, M., Ben-Avraham, Z., & Tibor, G. (1997). The subsidence history of the northern Hyblean plateau margin, southeastern Sicily. *Tectonophysics*, *282*(1–4), 277–289. https://doi.org/10.1016/S0040-1951(97)00228-X

Yousef, M., Moustafa, A. R., & Shann, M. (2010). Structural setting and tectonic evolution of offshore North Sinai, Egypt. *Geological Society, London, Special Publications*, *341*(1), 65–84. https://doi.org/10.1144/SP341.4

Zarcone, G., Petti, F. M., Cillari, A., Di Stefano, P., Guzzetta, D., & Nicosia, U. (2010). A possible bridge between Adria and Africa: New palaeobiogeographic and stratigraphic constraints on the Mesozoic palaeogeography of the Central Mediterranean area. *Earth-Science Reviews*, *103*(3–4), 154–162. https://doi.org/10.1016/j.earscirev.2010.09.005